NATIONAL ADVISORY COMMITTEE FOR AERONAUTICS

TECHNICAL NOTE 3662

THEORETICAL LOSS RELATIONS FOR LOW-SPEED TWO-DIMENSIONAL-CASCADE FLOW

By Seymour Lieblein and William H. Roudebush

Lewis Flight Propulsion Laboratory
Cleveland, Ohio

Washington
March 1956

NATIONAL ADVISORY COMMITTEE FOR AERONAUTICS

TECHNICAL NOTE 3662

THEORETICAL LOSS RELATIONS FOR LOW-SPEED TWO-DIMENSIONAL-CASCADE FLOW

By Seymour Lieblein and William H. Roudebush

SUMMARY

The relations between wake characteristics and total-pressure defect were theoretically analyzed for the incompressible flow across a two-dimensional cascade of compressor blades. Equations for total-pressure-loss coefficient both in an arbitrary downstream plane and in a plane far downstream where complete mixing has occurred were developed in terms of the wake momentum thickness and form factor at the arbitrary plane. Results indicated that the total-pressure-loss coefficient for unseparated flow varied almost directly with the ratio of wake momentum thickness to blade chord length and with the solidity, and inversely with the cosine of the air outlet angle.

Sample calculations indicated that the additional loss incurred in the mixing of the wake is a function primarily of the form factor of the wake at the start of the mixing, and also that the mixing loss may be a significant proportion of the loss at the trailing edge. The effect of trailing-edge thickness was indicated to be possibly significant for conventional compressor blade sections.

It was concluded from the analysis that the wake characteristics of momentum thickness and form factor constitute significant parameters for the presentation and correlation of two-dimensional-cascade loss data.

INTRODUCTION

It is a difficult task to predict and control losses in axial-flow-compressor design because of the complex three-dimensional nature of the loss phenomenon. For simplicity, the standard approach considers that the complete loss in compressor blade rows can be constructed by properly correcting blade-profile losses for three-dimensional effects. A necessary first step in such an analysis is the determination of the blade-profile loss. The basic blade-profile loss is considered to include the loss accrued in the mixing of the wake downstream of the blade.

The problem of theoretical loss estimation for blade profiles involves first, a determination of the boundary-layer characteristics on the blade surfaces and, second, a means of determining the total-pressure defect resulting from these boundary-layer characteristics. The first part of the problem has received considerable attention (e.g., refs. 1 and 2), although certain difficulties still remain. The second part of the problem, which is the concern of the present paper, has also been investigated in references 3 to 5. These references show that analytical relations between certain blade-wake boundary-layer characteristics and the resulting defect in total pressure can be established for cascade flow. The present paper continues the approach and presents a detailed theoretical analysis of cascade loss and wake relations in terms of wake momentum thickness and form factor. The analysis is directed specifically toward establishing simplified equations and considerations that may prove useful in the estimation of profile losses and in the correlation of experimental data in the low-speed two-dimensional cascade, which is the primary source of compressor blade-profile data.

The analysis is made for incompressible two-dimensional flow. Relations are obtained between the total-pressure defect and the wake characteristics at an arbitrary station between zero and about $1\frac{1}{2}$ chord lengths downstream of the trailing edge. Both the total-pressure defect up to the station and the defect for complete mixing are considered. From these relations, the various factors influencing the loss are determined and their relative effects are evaluated.

SYMBOLS

c	chord length, ft
H	form factor, δ^*/θ
K	pseudoenergy factor, k/θ
k	pseudoenergy thickness, ft
n	exponent in power velocity profile relation (table I)
P	total pressure, lb/sq ft
$\Delta\overline{P}$	mass-averaged decrease in total pressure, lb/sq ft
p	static pressure, lb/sq ft
s	distance along outlet streamline, ft
t	blade trailing-edge thickness, ft

$\hat{t}$ blade trailing-edge-thickness parameter, $\left(\frac{t}{c}\right)\frac{\sigma}{\cos \beta}$

V velocity, ft/sec

Y half blade spacing normal to axial direction measured from wake centerline (y = 0, fig. 1)

y coordinate normal to axial direction (fig. 1)

z coordinate in axial direction (fig. 1)

α angle of attack, deg

β air angle (angle between flow direction and axis), deg

δ full boundary-layer or wake thickness, ft

δ^* displacement thickness, ft

$\hat{\delta}$ full-thickness parameter, $\left(\frac{\delta}{c}\right)\frac{\sigma}{\cos \beta}$

θ momentum thickness, ft

$\hat{\theta}$ momentum-thickness parameter, $\left(\frac{\delta}{c}\right)\frac{\sigma}{\cos \beta}$

ρ mass density, lb-sec^2/ft^4

σ solidity, c/2Y

$\bar{\omega}_1$ total-pressure-loss coefficient for loss up to cascade measuring station, $\frac{(\Delta\bar{P})_2}{\frac{1}{2}\rho V_1^2}$

$\bar{\omega}_2$ total-pressure-loss coefficient for loss up to cascade measuring station, $\frac{(\Delta\bar{P})_2}{\frac{1}{2}\rho V_{0,2}^2}$

$\bar{\omega}_x^*$ total-pressure-loss coefficient for loss up to outlet plane based on air angle in outlet plane, $\frac{(\Delta\bar{P})_x}{\frac{1}{2}\rho V_1^2}\left(\frac{\cos \beta_x}{\cos \beta_1}\right)^2$

$\bar{\omega}_{\infty,x}^*$ total-pressure-loss coefficient for loss for complete mixing based on air angle in outlet plane, $\frac{(\Delta\bar{P})_\infty}{\frac{1}{2}\rho V_1^2}\left(\frac{\cos \beta_x}{\cos \beta_1}\right)^2$

Subscripts:

l	lower surface
min	minimum
t	plane of trailing edge
u	upper surface
x	arbitrary outlet plane 0 to $1\frac{1}{2}$ chord lengths downstream of trailing edge
y	normal to axial direction
z	axial direction
0	free stream
1	inlet
2	outlet measuring station (1/2 to 1 chord length downstream of trailing edge)
∞	far downstream where complete mixing has taken place

GENERAL CONSIDERATIONS

In subsonic two-dimensional-cascade flow, losses arise from the growth of boundary layers on the suction and pressure surfaces of the blades. These surface boundary layers then come together at the blade trailing edge to form the blade wake, as shown in figure 1. As a result of the formation of the surface boundary layers, a local defect in total pressure is created and a certain mass-averaged loss in total pressure occurs in the plane of the trailing edge.

Downstream of the trailing edge, a mixing takes place between the wake and the free-stream flow, and the wake is eventually reenergized through turbulent mixing. Inasmuch as a loss in total pressure is involved in the mixing process, the ultimate total pressure at a station far downstream where conditions have become uniform will be less than the average total pressure at the blade trailing edge. This difference in total pressure is referred to as the mixing loss. The loss for complete mixing represents the total loss attributable to a given wake profile in the two-dimensional cascade.

Although the losses encountered in the flow over the blade profiles of a two-dimensional cascade can be expressed in various ways (e.g., drag coefficient, wake coefficient, total-pressure defect, entropy rise), it is ultimately desirable, for the determination of compressor blade-row efficiency and entropy gradients, to determine the loss in total pressure involved in the flow. This cannot as yet be done theoretically because of the current inability to determine accurately the turbulent viscous flow across blade sections. However, wherever the flow field is separated clearly into a wake region and a free-stream region (as in fig. 1), mathematical relations can be developed to express the loss in total pressure as a function of the local properties of the wake. Although this does not solve the problem of loss estimation (the boundary-layer and wake parameters cannot be calculated accurately in all cases), the approach does point out the relative influence of the various geometric and aerodynamic factors on the resulting loss in total pressure.

In cascade loss analysis there are two stations of particular interest: (1) the plane of the trailing edge and (2) the usual cascade measuring station (about 1/2 to 1 chord length downstream of the trailing edge). Consideration of cascade losses in terms of the wake characteristics at the blade trailing edge is desirable, because ultimately, in the development of effective cascade flow theory (potential flow and boundary-layer theory), it should be possible to compute satisfactorily the surface boundary-layer characteristics (momentum thickness and form factor) at the blade trailing edge. Significant developments along these lines are represented, for example, by reference 6. A study of the significant parameters determining the loss at the cascade measuring station is also necessary so that the available experimental data can best be analyzed and correlated.

The analysis starts with a development of the general equations for the loss in total pressure up to an arbitrary outlet station and for the loss in total pressure after complete mixing. These equations are expressed in terms of the wake characteristics of momentum thickness and form factor at the arbitrary outlet location. The application of these relations to two specific outlet locations, the plane of the trailing edge and the usual cascade measuring station, is then discussed.

BASIC EQUATIONS

Assumptions

The theoretical development of cascade loss relations is based on the fundamental premise that, for short distances downstream of conventional cascades (say, up to about $1\frac{1}{2}$ to 2 chord lengths), the outlet flow in a plane normal to the axial direction of the cascade (fig. 1)

can be divided into a wake region where gradients in total pressure occur and a free-stream region where the total pressure is essentially constant. In conjunction with this premise, the following specific assumptions are made: (1) the flow is two-dimensional and incompressible, (2) the inlet flow is uniform across the blade spacing (y-direction), (3) the outlet static pressure and flow angle are constant across the entire blade spacing, (4) the outlet total pressure is constant in the free stream outside the wake, and (5) the outlet free-stream total pressure is equal to the inlet total pressure. Under these assumptions, the variations in outlet velocity and pressure in an arbitrary plane normal to the axial direction will appear as shown in figure 2.

The validity of these assumptions varies with distance downstream of the blade trailing edge. General cascade experience indicates that they are sufficiently valid in the region covered by the present analysis to provide results that are qualitatively correct. These assumptions have frequently been employed in cascade loss analyses (refs. 3 to 5).

Loss at Outlet Station

Development of equations. - For an outlet plane located at any distance between 0 and about $1\frac{1}{2}$ chord lengths downstream of the blade trailing edge, the mass-averaged loss in total pressure between the cascade inlet plane (subscript 1) and the general outlet plane (subscript x) is given by

$$(\Delta\bar{P})_x = P_1 - \frac{\int_{-Y}^{Y} \rho V_{z,x} P_x dy}{\int_{-Y}^{Y} \rho V_{z,x} dy} \tag{1}$$

With free-stream total pressure assumed constant between station 1 and the general outlet station, the loss across the cascade is given by the defect in total pressure in the outlet plane as

$$(\Delta\bar{P})_x = \frac{\int_{-Y}^{Y} \rho V_{z,x}(P_{0,x} - P_x) dy}{\int_{-Y}^{Y} \rho V_{z,x} dy} \tag{2}$$

From the Bernoulli equation for incompressible flow,

$$P = p + \frac{1}{2}\rho V^2 \tag{3}$$

Then, inasmuch as static pressure is assumed constant across the entire blade spacing in the y-direction, equation (2) can be expressed as

$$(\Delta\bar{P})_x = \frac{\frac{\rho}{2}\int_{-Y}^{Y}(V_{0,x}^2 - V_x^2)V_x \cos\beta_x dy}{\int_{-Y}^{Y} V_x \cos\beta_x dy} \tag{4}$$

With outlet angle β_x constant across the blade spacing, equation (4) can be given, after expressing the velocities in terms of ratios, as

$$(\Delta\bar{P})_x = \frac{\frac{1}{2}\rho V_{0,x}^2 \int_{-Y}^{Y}\left[1 - \left(\frac{V_x}{V_{0,x}}\right)^2\right]\left(\frac{V_x}{V_{0,x}}\right)dy}{2Y - \int_{-Y}^{Y}\left(1 - \frac{V_x}{V_{0,x}}\right)dy} \tag{5}$$

Actually, since $V_x = V_{0,x}$ in the free stream, the limits of integration in equation (5) can be restricted to the limits of the wake region extending from $-\delta_{l,y}$ to $\delta_{u,y}$ (see fig. 2).

Since the momentum thickness is a basic parameter in all simplified boundary-layer theory, it is desirable to express equation (5) in terms of this parameter. This can be accomplished by expanding the integral in the numerator to yield

$$(\Delta\bar{P})_x = \frac{\frac{1}{2}\rho V_{0,x}^2}{2Y - \int_{-\delta_{l,y}}^{\delta_{u,y}}\left(1 - \frac{V_x}{V_{0,x}}\right)dy}\left\{\int_{-\delta_{l,y}}^{\delta_{u,y}}\left(1 - \frac{V_x}{V_{0,x}}\right)\left(\frac{V_x}{V_{0,x}}\right)dy + \int_{-\delta_{l,y}}^{\delta_{u,y}}\left(1 - \frac{V_x}{V_{0,x}}\right)\left(\frac{V_x}{V_{0,x}}\right)^2 dy\right\} \tag{6}$$

The following definitions of wake characteristics are now made:

Displacement thickness:

$$\delta_y^* = \int_{-\delta_{l,y}}^{\delta_{u,y}}\left(1 - \frac{V}{V_0}\right)dy \tag{7a}$$

Momentum thickness:

$$\theta_y = \int_{-\delta_{l,y}}^{\delta_{u,y}} \left(1 - \frac{V}{V_0}\right)\left(\frac{V}{V_0}\right) dy \tag{7b}$$

Pseudoenergy thickness:

$$k_y = \int_{-\delta_{l,y}}^{\delta_{u,y}} \left(1 - \frac{V}{V_0}\right)\left(\frac{V}{V_0}\right)^2 dy \tag{7c}$$

The integrals appearing in equations (7a) and (7b) are similar to the standard boundary-layer-thickness parameters, except that the integration path is normal to the cascade axial direction instead of being normal to the flow direction. These modified thickness parameters are designated by the subscript y. Substituting equations (7) into equation (6) then yields

$$(\Delta\bar{P})_x = \frac{1}{2}\rho V_{0,x}^2 \frac{\left(\frac{\theta_y}{2Y}\right)_x + \left(\frac{k_y}{2Y}\right)_x}{1 - \left(\frac{\delta_y^*}{2Y}\right)_x} \tag{8}$$

In equation (8), $V_{0,x}$ is not completely independent of the wake formation. The presence of the wake displacement thickness causes an acceleration of the free-stream flow which is reflected as an increase in the $V_{0,x}^2$ term. This point can be brought out more clearly by expressing the loss in terms of the inlet dynamic head. From continuity, for uniform inlet conditions

$$2Y\ \rho V_1 \cos\beta_1 = \int_{-Y}^{Y} \rho V_x \cos\beta_x dy \tag{9}$$

Dividing both sides of equation (9) by $\rho V_{0,x}\cos\beta_x$ and adding and subtracting $2Y$ to the right side of the equation give

$$2Y \frac{V_1}{V_{0,x}} \frac{\cos\beta_1}{\cos\beta_x} = 2Y - \int_{-\delta_{l,y}}^{\delta_{u,y}} \left(1 - \frac{V_x}{V_{0,x}}\right) dy$$

or

$$V_{0,x} = \frac{V_1\left(\frac{\cos \beta_1}{\cos \beta_x}\right)}{1 - \left(\frac{\delta_y^*}{2Y}\right)_x} \tag{10}$$

Substitution of equation (10) into equation (8) then yields

$$(\Delta\bar{P})_x = \frac{1}{2}\rho V_1^2 \left(\frac{\cos \beta_1}{\cos \beta_x}\right)^2 \frac{\left(\frac{\theta_y}{2Y}\right)_x + \left(\frac{k_y}{2Y}\right)_x}{\left[1 - \left(\frac{\delta_y^*}{2Y}\right)_x\right]^3} \tag{11}$$

The total-pressure loss, in this form, is a more explicit function of the wake characteristics. Specifically, it is revealed that the mass-averaged loss in total pressure in any outlet plane will depend on the inlet dynamic head, the inlet and outlet air angles, and the ratio to blade spacing of the wake momentum, displacement, and pseudoenergy thicknesses in the outlet plane.

For analysis purposes in investigating the relation between total-pressure loss and wake characteristics, it is convenient to use a loss coefficient defined as

$$\bar{\omega}_x^* = \frac{(\Delta\bar{P})_x}{\frac{1}{2}\rho V_1^2}\left(\frac{\cos \beta_x}{\cos \beta_1}\right)^2 \tag{12}$$

which differs in the term $(\cos \beta_x/\cos \beta_1)^2$ from the more customary definition of loss coefficient given by

$$\bar{\omega}_1 = \frac{(\Delta\bar{P})_x}{\frac{1}{2}\rho V_1^2}$$

The definition of loss coefficient given by equation (12) will be used throughout the present analysis. Thus, equation (11) can be expressed as

$$\bar{\omega}_x^* = \frac{\left(\frac{\theta_y}{2Y}\right)_x + \left(\frac{k_y}{2Y}\right)_x}{\left[1 - \left(\frac{\delta_y^*}{2Y}\right)_x\right]^3} \tag{13}$$

Applied form. - For use in the analysis of cascade and compressor loss data, it is desirable that the derived loss equations be put in the most applicable and significant forms. Several factors can be considered in this respect.

In the previous loss equations, it is to be noted that the wake thicknesses involved are defined in the plane normal to the axial direction. However, inasmuch as one of the purposes of the development is to permit the calculation of total-pressure losses resulting from the blade boundary-layer growth, it would be well to express the loss equations in terms of the conventional wake thicknesses normal to the free-stream flow. This can be accomplished by assuming that the thickness of the wake or boundary layer in any plane (i.e., normal to the blade surface or normal to the outlet flow direction) can be related to the thickness in the plane normal to the axis through the cosine of the angle between the plane in question and the normal plane. This relationship will be valid as long as the axial gradients of flow in the wake are not large. Thus, in terms of wake thickness normal to the outlet flow at angle β, it is assumed that with little error

$$\left.\begin{aligned} \delta &= \delta_y \cos \beta \\ \delta^* &= \delta_y^* \cos \beta \\ k &= k_y \cos \beta \\ \theta &= \theta_y \cos \beta \end{aligned}\right\} \tag{14}$$

Use will also be made of the definitions of wake form factor H and pseudoenergy factor K given respectively by

$$H = \frac{\delta^*}{\theta} \tag{15a}$$

$$K = \frac{k}{\theta} \tag{15b}$$

Furthermore, it is desirable to express the blade spacing in terms of the blade solidity σ and chord length c, where $\sigma = c/2Y$. Thus, from equations (14), (15), and the solidity relation, equation (13) becomes

$$\overline{\omega}_x^* = \left(\frac{\theta}{c}\right)_x \frac{\sigma}{\cos \beta_x} \frac{1 + K_x}{\left[1 - \left(\frac{\theta}{c}\right)_x \frac{\sigma H_x}{\cos \beta_x}\right]^3} \tag{16}$$

With the further definition of the wake momentum-thickness parameter $\hat{\theta}$ given by

$$\hat{\theta}_x = \left(\frac{\theta}{c}\right)_x \frac{\sigma}{\cos \beta_x} \tag{17}$$

equation (16) for the loss coefficient becomes

$$\bar{\omega}_x^* = \hat{\theta}_x \frac{1 + K_x}{(1 - \hat{\theta}_x H_x)^3} \tag{18}$$

As a simplification, it would be desirable if the pseudoenergy factor K could be expressed in terms of the form factor H. Accordingly, values of K were investigated for several representative analytical variations of velocity in the wake, as shown by the half-wake profiles in figure 3. (It is assumed that the velocity profiles in fig. 3 are symmetrical about the point of minimum velocity at $y/\frac{\delta}{2} = 0$.) The power velocity profile, with minimum velocity ratio $V_{min}/V_0 = 0$ (fig. 3(a)), represents the form of the wake at the trailing edge. The other velocity distributions are intended to represent possible wake profiles some distance downstream where some mixing has occurred and $V_{min}/V_0 > 0$. The thickness $\frac{\delta}{2}$ of the half wake for the error-curve profile (fig. 3(e)) was arbitrarily established as the value of $y/\frac{\delta}{2}$ at which $V/V_0 = 0.99$. (The integrated values are those of the definite integrals obtained from allowing $y/\frac{\delta}{2} \to \infty$.) Equations for V/V_0 for the profiles are given in table I.

Computed values of K determined from equations (7b), (7c), and (15b) are shown as a function of H (computed from eqs. (7a), (7b), and (15a)) for the various analytical profiles in figure 4. Variations in K and H were obtained for the power profile by varying the exponent n and for the other profiles by varying the minimum velocity ratio V_{min}/V_0. The equations for K obtained for the various profiles are given in table I. Also shown in the figure are values computed from experimental wake-profile data obtained in references 7 to 10. The data of references 7 to 9 were taken approximately 1/2 chord length downstream of the blades, and for reference 10, about 0.02 chord length.

Figure 4 shows that profile form should not be a significant factor in the K-H relation. For values of H up to about 1.4, a maximum difference of less than $1\frac{1}{2}$ percent is indicated for the quantity (1 + K),

and therefore for $\overline{\omega}_x^*$ in equation (18) for the various profiles considered. As will be indicated later, higher values of H, for which maximum differences in (1 + K) up to about 3 percent are indicated, will generally occur only in the trailing-edge region where V_{min}/V_0 may be near zero. In view of these considerations, the K-H variation given by the power velocity profile was adopted as the simplest acceptable approximation to the general K-H relation for use in the loss equation. This selection is reasonably substantiated by the limited experimental data presented.

With K for the power velocity profile given by

$$K = \frac{H + 1}{3H - 1} \tag{19}$$

the equation for the loss coefficient from equations (18) and (19) becomes

$$\overline{\omega}_x^* = 2\hat{\theta}_x \frac{\frac{2H_x}{3H_x - 1}}{(1 - \hat{\theta}_x H_x)^3} \tag{20}$$

It is thus established that the total-pressure-loss coefficient (as defined by eq. (12)) in a plane downstream of the trailing edge is a function of the wake momentum-thickness parameter (as defined by eq. (17)) and the wake form factor.

A plot of the calculated variation of $\overline{\omega}_x^*$ against $\hat{\theta}_x$ (from eq. (20)) for a range of values of H_x from 1.2 to 2.6 is shown in figure 5. The plot of figure 5 reveals that $\overline{\omega}_x^*$ is only a secondary function of H. In fact, for values of $\hat{\theta}_x \leq$ about 0.07 and values of $H_x \leq$ about 2.0 (representative trailing-edge values for unstalled flow), the loss coefficient is essentially independent of the value of H_x.

Loss for Complete Mixing

The complete loss in total pressure attributable to a cascade blade row is measured only at a station (subscript ∞) sufficiently far downstream for the flow to again become uniform across the blade spacing as shown in figure 6. Since the flow is uniform in the y-direction both far upstream and far downstream, the mass-averaged defect in total pressure is given by

$$(\Delta\overline{P})_\infty = P_1 - P_\infty = P_{0,x} - P_\infty \tag{21}$$

It is now desired to express $(\Delta\bar{P})_\infty$ in terms of wake and flow characteristics in the general outlet plane. To do this, it is necessary to express the pressures in equation (21) in terms of velocities. The conversion to velocities is achieved through the application of the Bernoulli equation and the equations for conservation of momentum in the axial and tangential directions for the flow envelope bounded by the streamlines a-a and b-b and by the outlet and far-downstream planes in figure 6. The details of the development are presented in the appendix.

With the definition of the loss coefficient for complete mixing based on the air angle in the general outlet plane given by

$$\bar{\omega}^*_{\infty,x} = \frac{(\Delta\bar{P})_\infty}{\frac{1}{2}\rho V_1^2}\left(\frac{\cos\beta_x}{\cos\beta_1}\right)^2 \tag{22}$$

it is shown in the appendix that

$$\bar{\omega}^*_{\infty,x} = \frac{2\hat{\theta}_x}{(1-\hat{\theta}_x H_x)^2}\left\{1 + \frac{\hat{\theta}_x}{2}\left[H_x^2 - \sin^2\beta_x\left(H_x - \frac{1}{1-\hat{\theta}_x H_x}\right)^2\right]\right\} \tag{23}$$

The loss coefficient for complete mixing is thus a function of the air angle as well as of the wake momentum-thickness parameter and the form factor in the outlet plane.

The calculated variation of $\bar{\omega}^*_{\infty,x}$ with $\hat{\theta}_x$ for a range of values of H_x from 1.0 to 2.6 and for β_x of 0° and 60° as obtained from equation (23) is plotted in figure 7. The figure shows that, unlike the case for the local loss coefficient in the outlet plane (fig. 5), the loss coefficient for complete mixing depends to a significant extent on the value of the wake form factor. The influence of the outlet air angle β_x, however, is small.

Mixing-Loss Ratio

An indication of the additional loss incurred by the complete mixing of the wake can be conveniently obtained from consideration of the mixing-loss ratio; that is, the ratio of the loss for complete mixing to the loss up to the outlet plane. From equations (23) and (18), the mixing-loss ratio is given, in terms of the wake characteristics in the outlet plane, by

$$\left(\frac{\bar{\omega}^*_\infty}{\bar{\omega}^*}\right)_x = \frac{2(1-\hat{\theta}_x H_x)}{1+K_x}\left\{1 + \frac{\hat{\theta}_x}{2}\left[H_x^2 - \sin^2\beta_x\left(H_x - \frac{1}{1-\hat{\theta}_x H_x}\right)^2\right]\right\} \tag{24}$$

A numerical evaluation of equation (24) in terms of H_x and $\hat{\theta}_x$ can be obtained through the use of the representative relation between K_x and H_x given by equation (19). A plot of the variation of mixing-loss ratio against H_x so obtained is shown in figure 8 for β_x of 0° and 60°. Figure 8 reveals the general observation that the mixing-loss ratio at a given outlet-plane location is determined primarily by the form factor of the wake in the outlet plane.

As H_x approaches 1.0 in figure 8, calculated values of mixing-loss ratio less than 1.0 are obtained for values of $\hat{\theta}_x$ greater than 0. This result is obtained mathematically because of the independent manner in which $\hat{\theta}_x$ and H_x are allowed to vary in the calculation. For an actual wake profile, $\hat{\theta}_x$ and H_x do not vary completely independently; and, at a value of H_x of 1.0, $\hat{\theta}_x$ must be zero. Values of mixing-loss ratio less than 1.00 in figure 8, therefore, represent regions of unreal flow.

The exact nature of the mixing-loss ratio as H_x approaches 1.0 can be demonstrated more clearly by examining the mixing-loss ratio of a given wake velocity profile. For the power velocity profile of figure 3(a), for example, K_x can be expressed in terms of H_x through equation (19), and $\hat{\theta}_x$ can be expressed in terms of H_x and the wake full thickness parameter $\hat{\delta}_x$, where

$$\hat{\delta}_x = \left(\frac{\delta}{c}\right)_x \frac{\sigma}{\cos \beta_x} \tag{25}$$

by

$$\hat{\theta}_x = \frac{\hat{\delta}_x}{H_x}\left(\frac{H_x - 1}{H_x + 1}\right) \tag{26}$$

Substitution of equations (19) and (26) into equation (24) then yields for the power velocity profile

$$\left(\frac{\bar{a}_\infty^*}{\bar{w}^*}\right)_x = \frac{3H_x - 1}{2H_x}\left[1 - \hat{\delta}_x\left(\frac{H_x - 1}{H_x + 1}\right)\right]\left(1 + \frac{\hat{\delta}_x}{2H_x}\left(\frac{H_x - 1}{H_x + 1}\right)\left\{H_x^2 - \sin^2\beta_x\left[H_x - \frac{1}{1 - \hat{\delta}_x\left(\frac{H_x - 1}{H_x + 1}\right)}\right]^2\right\}\right) \tag{27}$$

Plots of the variation of $(\overline{\omega}_{\infty}^{*}/\overline{\omega}^{*})_x$ with H_x and β_x for the power velocity profile are shown in figure 9 for a range of values of $\hat{\delta}_x$. (The value of $\hat{\delta}_x = 0.6$ corresponds approximately to $\hat{\theta}_x = 0.1$.) The convergence of the values of $(\overline{\omega}_{\infty}^{*}/\overline{\omega}^{*})_x$ to 1.0 as H_x approaches 1.0 is clearly indicated for all values of $\hat{\delta}_x$ in figure 9(a). The small effect of air outlet angle on mixing-loss ratio for unstalled flow ($H_x < 2.0$) is shown in figure 9(b).

Mixing-loss ratios were also determined for the other representative velocity profiles shown in figure 3. For a given wake velocity distribution, K can be expressed in terms of H, and θ can be expressed in terms of H and the wake full thickness δ. Equations for θ and K for the various wake profiles of figure 3 are given in table I. The substitution of the relations for K and θ in table I into equation (24) yields the mixing-loss ratio for the various profiles as a function of H_x, $\hat{\delta}_x$, and β_x in the general outlet plane. A comparative plot of the calculated variation of $(\overline{\omega}_{\infty}^{*}/\overline{\omega}^{*})_x$ with H_x for representative limiting values of $\hat{\delta}_x$ and β_x is shown in figure 10 for all five profiles. Figure 10 shows that the mixing-loss ratio may be essentially independent of the particular variation of the velocity in the wake.

Summary

In summary, the preceding analysis of the loss relations for the wake in an outlet plane located from 0 to about $1\frac{1}{2}$ chord lengths downstream of a cascade indicates that, for unstalled configurations, the total-pressure-loss coefficient (as defined by eq. (12)) up to the outlet plane is essentially a function of only the local wake momentum-thickness parameter (eq. (17)). The ratio of the total-pressure loss for complete mixing to the loss at the outlet plane depends primarily on the form factor of the wake in the outlet plane.

APPLICATION TO PLANE OF TRAILING EDGE

An outlet station of practical interest in cascade loss analyses in the plane of the blade trailing edge, where the blade-surface boundary layers come together to form the blade wake (station t, fig. 1). The development of loss equations for the plane of the trailing edge can permit the calculation of the loss in total pressure arising from the development of the boundary layers on the blade surfaces, as determined from blade boundary-layer theory.

Of all the assumptions stipulated for the general analysis in the arbitrarily located plane, perhaps the one concerning the constancy of the static pressure across the blade spacing may be most questionable in the plane of the trailing edge. It is recognized that static-pressure gradients will normally occur in the plane of the blade trailing edge, depending on the blade circulation and surface curvatures; and, as a consequence, the derived relations will not be an exact representation of the flow. At present, there is no available information concerning the effect of such gradients on the results of the simplified developments. It is believed, however, that the existence of the static-pressure gradients normally encountered in conventional unstalled cascade operation will not materially alter the principal conclusions and trends of variation established from an analysis based on uniform static pressure.

For simplicity, the case of zero blade trailing-edge thickness will be considered first.

Equations for Zero Trailing-Edge Thickness

In the plane of the trailing edge, under the assumptions of the analysis and the condition of no blade trailing-edge thickness, the variations of velocity and pressure in the y-direction will appear as shown in figure 11(a). The wake thicknesses at the trailing edge consist of the wake thicknesses of the upper- and lower-surface boundary layers, so that

$$\left.\begin{aligned} \delta_y &= \delta_{u,y} + \delta_{l,y} \\ \delta_y^* &= \delta_{u,y}^* + \delta_{l,y}^* \\ \theta_y &= \theta_{u,y} + \theta_{l,y} \\ H &= \frac{\delta_{u,y}^* + \delta_{l,y}^*}{\theta_{u,y} + \theta_{l,y}} \\ K &= \frac{k_{u,y} + k_{l,y}}{\theta_{u,y} + \theta_{l,y}} \\ \theta_y H &= \theta_{u,y} H_u + \theta_{l,y} H_l \end{aligned}\right\} \tag{28}$$

A similar set of equations can readily be established for thicknesses normal to the air angle β_t through the cosine of the angle β_t as in equations (14). The accuracy of this conversion to the normal wake

thicknesses in the plane of the trailing edge is perhaps not as good as it would be farther downstream, since the rates of change of the wake properties along the direction of the flow are greatest in the region of the trailing edge.

Loss at trailing edge. - The equation for loss coefficient in the plane of the trailing edge is then obtained from equation (18) as

$$\bar{\omega}_t^* = \hat{\theta}_t \frac{1 + K_t}{(1 - \hat{\theta}_t H_t)^3} \tag{29}$$

or, with the K-H relation of the power velocity profile (eq. (19)),

$$\bar{\omega}_t^* = 2\hat{\theta}_t \frac{\frac{2H_t}{3H_t - 1}}{(1 - \hat{\theta}_t H_t)^3} \tag{30}$$

where the θ and H values are determined as in equation (28).

The wake momentum thickness of equations (29) and (30) is normal to the air outlet angle in the plane of the trailing edge, which may not necessarily be equal to the mean of the angles of the tangents to the blade surfaces at the trailing edge. Strictly speaking, since the results of surface boundary-layer calculations generally yield boundary-layer properties normal to the blade surfaces, an adjustment for the differences between these angles should be made in the determination of the wake thickness values for use in equation (30). However, such a refinement is outside the accuracy of the present analysis.

For boundary-layer flow on blade surfaces, values of form factor H may generally be obtained from about 1.3 to about 2.0 to 2.6 when separation occurs. Furthermore, analysis of compressor cascade blade losses reveals that separation in the low-loss range of incidence-angle operation is indicated for values of wake momentum-thickness ratio (θ/c) greater than about 0.02. Thus, for unseparated flow, for a high value of solidity of about 1.75, and a high value of air outlet angle of about 60°, a momentum-thickness parameter $\hat{\theta}$ of less than about 0.07 is obtained. Most blade sections will operate at values of $\hat{\theta}$ considerably lower than 0.07 in their design regions of incidence angle. A practical range of blade operation can therefore be represented for conventional compressor cascades by values of H_t from about 1.3 to about 2.2 and by values of $\hat{\theta}_t$ up to about 0.07. In this range, according to figure 5, $\bar{\omega}_t^*$ will not be very sensitive to the value of H_t. Equation (30) can

then be simplified by taking $H_t = 1.6$ as a representative average value to give

$$\bar{\omega}_t^* = \frac{1.684\hat{\theta}_t}{(1 - 1.6\hat{\theta}_t)^3} \tag{31}$$

Loss for complete mixing. - The equation for the loss coefficient for complete mixing based on the wake characteristics at the trailing edge is obtained from equation (23) as

$$\bar{\omega}_{\infty,t}^* = \frac{2\hat{\theta}_t}{(1 - \hat{\theta}_t H_t)^2} \left\{ 1 + \frac{\hat{\theta}_t}{2} \left[H_t^2 - \sin^2 \beta_t \left(H_t - \frac{1}{1 - \hat{\theta}_t H_t} \right)^2 \right] \right\} \tag{32}$$

The plot of $\bar{\omega}_{\infty,x}^*$ against $\hat{\theta}_x$ in figure 7 shows that, for the practical range of values of $\hat{\theta}_t$ and H_t at the trailing edge, the influence of β_t will be very small. The effect of outlet angle can therefore be neglected by taking $\beta_t = 0$, so that, with little error, equation (32) can be simplified to

$$\bar{\omega}_{\infty,t}^* = 2\hat{\theta}_t \frac{1 + \frac{1}{2}\hat{\theta}_t H_t^2}{(1 - \hat{\theta}_t H_t)^2} \tag{33}$$

In the plane of the trailing edge, the power velocity profile is considered to be most representative of the velocity variation across the wake. Plots of the variation of the mixing-loss ratio $(\bar{\omega}_\infty^*/\bar{\omega}^*)_x$ against H_x and β_x for the power velocity profile are shown in figure 9. In the range of values of $H_t \geq 1.4$, the full thickness parameter $\hat{\theta}_t$ and the air outlet angle β_t exert only a secondary influence on the value of the mixing-loss ratio.

Effect of Trailing-Edge Thickness

Since practical blade sections are constructed with nonzero values of trailing-edge thickness, the question of the effect of this thickness on the total-pressure loss of the section is naturally raised. An accurate theoretical evaluation of the thickness effect is not currently feasible because of the complexity of the flow in the region of the trailing edge. Apparently, a rapid mixing between the flows along the upper and lower surfaces takes place immediately behind the trailing edge with accompanying large localized gradients of pressure and flow angle. The

precise nature of the flow in the trailing-edge region is expected to depend on the shape of the trailing edge (i.e., whether the trailing edge is blunt or rounded). At any rate, the presence of a blade trailing-edge thickness will affect the loss in total pressure because of the creation of additional mixing losses.

It is possible, under the assumptions of the present analysis, to determine the loss attributable to blade trailing-edge thickness by considering the flow immediately downstream of the trailing edge to be a "dead-air" region. The additional loss will thus appear in the form of a dumping loss. As indicated previously, the precise nature of the trailing-edge flow is too uncertain for the present qualified analysis to be expected to produce accurate estimates of the trailing-edge-thickness effect. However, the trends determined by this analysis should be correct.

According to the simplified picture of the trailing-edge effect, the variations of velocity and pressure in the y-direction immediately behind the trailing edge will appear as shown in figure 11(b). The trailing-edge thickness appears only as an effective increase in the wake full and displacement thicknesses, so that, for a trailing-edge thickness t,

$$\frac{\delta^*}{\theta} = \frac{\delta_u^* + \delta_l^* + t}{\theta_u + \theta_l} = H + \frac{t}{\theta} \tag{34}$$

Accordingly, the approximate equation for the loss coefficient for complete mixing can be obtained by replacing H_t in equation (33) by $H_t + \hat{t}/\hat{\theta}_t$ to give

$$\bar{\omega}_{\infty,t}^* = 2\hat{\theta}_t \frac{1 + \frac{1}{2}\hat{\theta}_t\left(H_t + \frac{\hat{t}}{\hat{\theta}_t}\right)^2}{\left[1 - \hat{\theta}_t\left(H_t + \frac{\hat{t}}{\hat{\theta}_t}\right)\right]^2} \tag{35}$$

where the trailing-edge thickness parameter $\hat{t}$ is defined as

$$\hat{t} = \left(\frac{t}{c}\right)\frac{\sigma}{\cos \beta_t} \tag{36}$$

and H_t and $\hat{\theta}_t$ are as before.

In order to examine the effect of trailing-edge thickness on the loss for complete mixing, the ratio of loss coefficient with trailing-edge

thickness $\bar{\omega}_{\infty}^{*}$ (eq. (35)) to the loss coefficient for zero trailing-edge $(\bar{\omega}_{\infty}^{*})_{\hat{t}=0}$ (eq. (33)) is established as

$$\frac{\bar{\omega}_{\infty}^{*}}{(\bar{\omega}_{\infty}^{*})_{\hat{t}=0}} = \frac{1 + \frac{1}{2}\hat{\theta}_t\left(H_t + \frac{\hat{t}}{\theta_t}\right)^2}{1 + \frac{1}{2}\hat{\theta}_t H_t^{\,2}} \left[\frac{1 - \hat{\theta}_t H_t}{1 - \hat{\theta}_t\left(H_t + \frac{\hat{t}}{\hat{\theta}_t}\right)}\right]^2 \tag{37}$$

Equation (37) is based on the assumption that $\hat{\theta}_t$ and H_t (obtained from the surface boundary-layer characteristics) are unaffected by changes in the blade trailing-edge thickness. A plot of the calculated variation of the loss ratio of equation (37) against trailing-edge-thickness parameter is shown in figure 12 for a range of values of $\hat{\theta}_t$ and H_t.

The results of figure 12 indicate that the percentage increase in loss due to mixing can be significant for large values of the trailing-edge-thickness parameter. For conventional compressor blades with trailing-edge-thickness ratios (t/c) of about 0.01 or 0.02 (and therefore for $\hat{t}$ up to about 0.035 or 0.070), the representative additional loss, according to figure 12, could be of the order of 15 to 55 percent. Although the loss magnitudes obtained by this simplified analysis are certainly questionable, the figure does indicate that definite advantages may be gained by maintaining trailing-edge thicknesses as small as possible. Similar results of the trailing-edge-thickness effect were obtained in references 3 and 11.

Discussion

The application of the derived loss equations to the plane of the trailing edge permits the calculation of the cascade loss in total pressure once the momentum thickness and form factor of the blade-surface boundary layers at the trailing edge are known. A completely theoretical determination of cascade losses can therefore be made on the basis of cascade boundary-layer theory and the trailing-edge loss relations presented herein. The reduced sensitivity of the loss coefficient to variations in H_t indicates that great accuracy in the theoretical determination of the boundary-layer values of H_t is not essential.

Because of the necessary assumptions involved in the developments, the loss equations are expected to be most accurate for the case of zero or nearly zero blade trailing-edge thickness. Further information concerning the nature of the flow and boundary-layer characteristics in the immediate vicinity of the blade trailing-edge region in the case of positive trailing-edge thickness is desirable.

APPLICATION TO PLANE OF MEASURING STATION

In the previous section, the loss equations were expressed in terms of the wake characteristics in the plane of the trailing edge. As such, they presumed a knowledge of the growth of the boundary layers on the blade surfaces. In most cases of cascade investigations, however, the losses are measured in a plane a short distance (say, from about 1/2 to 1 chord length) downstream of the cascade (station 2, fig. 1). At such distances, some mixing of the wake has already taken place and the minimum velocity in the wake is no longer zero. General cascade experience indicates that the wakes of conventional cascade configurations are clearly defined at the usual measuring-station locations and that $P_{0,2} = P_1$. Thus, the loss developments for the measuring station are expected to be more valid than at the trailing edge because of the greater uniformity of the static pressure in the y-direction and the smaller variation of the wake properties along the flow direction as distance behind the blade is increased.

The variations of velocity and pressure along the y-direction in the plane of the measuring station will appear as in figure 2. At the measuring station, the wake can no longer be divided specifically into its three components (suction-surface boundary layer, pressure-surface boundary layer, and trailing-edge thickness).

Equations

The equations for loss coefficient up to the measuring station, for loss coefficient for complete mixing, and for mixing-loss ratio expressed in terms of wake characteristics in the plane of the measuring station are obtained from the respective general equations (eqs. (20), (23), and (24)) by replacing the subscript x with the subscript 2 for the pertinent quantities involved. Simplifications of these equations can be obtained from consideration of the values of form factor H generally observed at the measuring station.

It is known that wake form factor decreases with distance downstream of the trailing edge and asymptotically approaches a value of 1.0. Experimental variations of wake form factor with distance downstream (expressed as the ratio s/c of distance along the wake to the airfoil chord length) for low-speed isolated and cascade airfoils are shown in figure 13. Apparently the decrease in H with distance is quite rapid. According to figure 13, values of H_2 between 1.0 and 1.2 should represent practical limits for a measuring-station location between 1/2 and 1 chord length behind the blade.

For the loss coefficient in the plane of the measuring station (eq. (20)), figure 5 shows that the dependency of $\overline{\omega}_2^*$ on H_2 is slight in the range $1.0 \leq H_2 < 1.2$. For practical purposes, an average value of

H_2 of 1.1 may be taken, so that, with negligible error, the equation for the loss coefficient at the measuring station can be given as

$$\bar{\omega}_2^* = \frac{1.912\hat{\theta}_2}{(1 - 1.1\hat{\theta}_2)^3} \tag{38}$$

For values of $H_2 < 1.2$, the effect of air outlet angle β_2 on the loss for complete mixing in the measuring plane essentially vanishes (fig. 7), so that, from equation (23),

$$\bar{\omega}_{\infty,2}^* = 2\hat{\theta}_2 \frac{1 + \frac{1}{2}\hat{\theta}_2 H_2^2}{(1 - \hat{\theta}_2 H_2)^2} \tag{39}$$

If desirable, an average value of $H_2 = 1.1$ may also be used in the equation for the loss for complete mixing.

According to the results of the mixing-loss-ratio calculations (figs. 8 and 9), for $1.0 \leq H_2 < 1.2$ in the measuring plane, very little additional loss will accrue as a result of any further mixing of the wake. Apparently, for a measuring station located from 1/2 to 1 chord length downstream of the blade trailing edge, a considerable part of the wake mixing loss has already occurred.

Comparison with Experiment

The accuracy of the loss equation in predicting the magnitude of the loss coefficient for a given value of wake momentum-thickness ratio was evaluated for the available experimental wake velocity-distribution data at the usual measuring station (refs. 7 to 10, e.g.). Integrations of the low-speed experimental wake-velocity profiles of the blade sections of references 7 to 10 were conducted to determine the wake momentum thickness, the wake form factor, and the mass-averaged total-pressure loss in the plane of the measuring station.

Since the experimental wake profiles in the references are plotted in terms of the local values of $V_2/V_{0,2}$ or $(P_{0,2} - P_2)\Big/\frac{1}{2}\rho V_{0,2}^2$, it is more convenient for comparison purposes to use a loss coefficient based on outlet dynamic head, such that by definition

$$\bar{\omega}_2 = \frac{(\Delta\bar{P})_2}{\frac{1}{2}\rho V_{0,2}^2} \tag{40}$$

where $(\Delta\bar{P})_2$ is the integrated mass-averaged loss in total pressure in the measuring plane (eq. (2)). The theoretical relation between loss coefficient $\bar{\omega}_2$ and the wake characteristics is obtained from equations (10) and (12) as

$$\bar{\omega}_2 = \frac{(\Delta\bar{P})_2}{\frac{1}{2}\rho V_1^2}\left(\frac{\cos\beta_2}{\cos\beta_1}\right)^2(1 - \hat{\theta}_2 H_2)^2 = \bar{\omega}_2^*(1 - \hat{\theta}_2 H_2)^2 \tag{41}$$

3559

so that, from equation (20),

$$\bar{\omega}_2 = 2\hat{\theta}_2 \frac{\frac{2H_2}{3H_2 - 1}}{1 - \hat{\theta}_2 H_2} \tag{42}$$

For the usual measuring-station location (s/c = 0.5 to 1), with $H_2 = 1.1$,

$$\bar{\omega}_2 = \frac{1.912\hat{\theta}_2}{1 - 1.1\hat{\theta}_2} \tag{43}$$

Loss coefficients were determined in two ways: first, by using the actual measured value of H_2 in equation (42), and secondly by using the representative value of $H_2 = 1.1$ as in equation (43)(applicable only within values of $s/c = 0.5$ to 1). Calculated and integrated values of $\bar{\omega}_2$ for these data are compared in the following table:

Blade section	Ref.	s/c	H_2	Integ. $(\theta/c)_2$	Integ. $\bar{\omega}_2$ (eq. (40))	Calc. $\bar{\omega}_2$ (eq. (42), actual H_2)	Calc. $\bar{\omega}_2$ (eq. (43), $H_2 = 1.1$)
Compressor blade, $\alpha = 15^\circ$	7	0.56	1.12	0.0151	0.0330	0.0338	0.0342
Compressor blade, $\alpha = 25^\circ$	7	.52	1.13	.0130	.0269	.0271	.0276
Thin turning vane	8	.50	1.10	.00250	.0309	.0309	.0309
Thick turning vane	8	.50	1.14	.00506	.0591	.0583	.0591
Compressor blade	9	.55	1.16	.00860	.0178	.0177	.0181
Compressor blade	10	.02	1.51	.0163	.0287	.0287	(.0319)

The close agreement between measured and calculated values of $\bar{\omega}_2$ indicates the validity of the K-H relation for these limited data.

Discussion

The establishment of relations between the total-pressure loss and the wake characteristics in the plane of the measuring station suggests several considerations in the empirical prediction of cascade losses and in the analysis of experimental cascade loss data. Since the total-pressure-loss coefficient depends primarily on the wake momentum-thickness parameter $\hat{\theta}_2 = \left(\frac{\theta}{c}\right)_2 \frac{\sigma}{\cos \beta_2}$, three major quantities are contained in the loss prediction, namely, the momentum-thickness ratio θ/c, the solidity σ, and the air outlet angle β_2. The quantities σ and β_2 depend primarily on the cascade geometry, so that the principal aerodynamic factor involved is the wake momentum-thickness ratio θ/c (and to a considerably smaller extent, the wake form factor). If generalized correlations of wake momentum-thickness ratio can be obtained in terms of the basic influencing parameters involved (e.g., velocity diffusion, Reynolds number, Mach number, etc.), the use of these correlations, in conjunction with the geometric characteristics of a particular cascade configuration could then form the basis of a loss prediction procedure according to the equations presented herein (eqs. (20) and (23)). The desirability of expressing cascade loss data in terms of wake momentum-thickness ratio is hereby indicated.

To date, experimental loss data have not generally been presented in terms of wake momentum-thickness ratio. However, it should be possible to convert the available data expressed in terms of other loss parameters (e.g., drag coefficient, total-pressure-loss coefficient, etc.) to corresponding values of wake momentum-thickness ratio. For example, a frequently used cascade loss parameter is the loss coefficient $\bar{\omega}_1$, defined, in terms of the symbols used in this report, by

$$\bar{\omega}_1 = (\Delta \bar{P})_2 \Big/ \frac{1}{2} \rho V_1^2$$

From equations (12) and (20),

$$\bar{\omega}_1 = \bar{\omega}_2^* \left(\frac{\cos \beta_1}{\cos \beta_2}\right)^2 = 2\hat{\theta}_2 \left(\frac{\cos \beta_1}{\cos \beta_2}\right)^2 \frac{\frac{2H_2}{3H_2 - 1}}{(1 - \hat{\theta}_2 H_2)^3} \tag{44}$$

or, since $\hat{\theta}_2 = \left(\frac{\theta}{c}\right)_2 \frac{\sigma}{\cos \beta_2}$,

$$\left(\frac{\theta}{c}\right)_2 = \frac{\bar{\omega}_1}{2} \frac{\cos \beta_2}{\sigma} \left(\frac{\cos \beta_2}{\cos \beta_1}\right)^2 \left(\frac{3H_2 - 1}{2H_2}\right) \left[1 - \left(\frac{\theta}{c}\right)_2 \frac{H_2 \sigma}{\cos \beta_2}\right]^3 \tag{45}$$

(In eq. (45), an iteration solution is required because of the high order to which θ/c appears.) Strictly speaking, the accurate solution of equation (45) requires a knowledge of the wake form factor. However, for practical purposes, as was indicated previously, a representative average value of H_2 may be satisfactorily used (say, an H_2 of about 1.1) in the calculations. (Similar relations can be developed for $(\theta/c)_2$ in terms of loss coefficients based on outlet dynamic head, eq. (42)).

SUMMARY OF RESULTS

Simple approximate equations have been developed to relate total-pressure loss in an incompressible plane cascade flow to the characteristics of the wake in a plane downstream of the blade trailing edge. Both the loss up to the plane and the complete loss after mixing have been expressed in terms of the characteristics of the wake in the plane. It was found that, for unseparated flow, the total-pressure-loss coefficient was primarily a direct function of the wake momentum-thickness ratio and the blade solidity and an inverse function of the cosine of the air outlet angle. A secondary factor in the determination of the loss coefficient was the value of the wake form factor H.

Application of the loss relations to the plane of the blade trailing edge indicated that, if the blade-surface boundary-layer momentum thickness and form factor at the trailing edge can be determined for a given cascade configuration, the corresponding loss in total pressure can be calculated according to the relations developed herein. From the theoretical developments, it was shown that, for conventional values of compressor blade trailing-edge thickness, the contribution of the trailing-edge thickness to the total loss may be significant. It was also shown that the additional loss resulting from the mixing of the wake can be a considerable percentage of the loss incurred at the trailing edge, depending upon the initial value of the wake form factor.

In a similar manner, the loss up to the usual cascade measuring station located from about 1/2 to 1 chord length downstream of the blade and the loss after complete mixing have been expressed in terms of the wake characteristics at the measuring station. In view of the small values of H indicated to occur at the measuring station, particularly simple relations were obtained for the measuring station showing the loss coefficient to vary effectively only with the wake momentum-thickness ratio, the solidity, and the air outlet angle.

It was concluded from the analysis that the wake characteristics of momentum-thickness ratio and form factor constitute significant parameters for the prediction of cascade losses and for the presentation and correlation of two-dimensional-cascade data. The developments also provide a means for computing the wake momentum-thickness ratio from reported values of loss coefficient.

Lewis Flight Propulsion Laboratory
National Advisory Committee for Aeronautics
Cleveland, Ohio, January 23, 1956

APPENDIX - LOSS COEFFICIENT FOR COMPLETE MIXING

The mass-averaged loss in total pressure between the inlet station (station 1, fig. 6) and the far-downstream station (station ∞, fig. 6) where the wake has been completely mixed is given by

$$(\Delta\bar{P})_\infty = P_1 - P_\infty$$

or, since $P_1 = P_{0,x}$ where the wake is well-defined (0 to about $1\frac{1}{2}$ chord lengths downstream of the cascade),

$$(\Delta\bar{P})_\infty = P_{0,x} - P_\infty \tag{21}$$

For conservation of momentum in the axial direction (fig. 6)

$$\int_{-Y}^{Y} \rho V_{z,x}^2 dy + 2Yp_x = 2Y\rho V_{z,\infty}^2 + 2Yp_\infty \tag{A1}$$

Substituting for P_x and p_∞ through the Bernoulli equation (eq. (3)) in equation (A1) gives

$$P_{0,x} - P_\infty = \rho V_{z,\infty}^2 - \frac{1}{2}\rho V_\infty^2 + \frac{1}{2}\rho V_{0,x}^2 - \frac{1}{2Y}\int_{-Y}^{Y} \rho V_{z,x}^2 dy$$

or

$$(\Delta\bar{P})_\infty = \frac{1}{2}\rho V_{0,x}^2 + \frac{1}{2}\rho V_{z,\infty}^2\left(2 - \frac{1}{\cos^2\beta_x}\right) - \frac{1}{2Y}\int_{-Y}^{Y} \rho V_{z,x}^2 dy \tag{A2}$$

The problem now is to express $V_{z,\infty}$ and $\cos\beta_\infty$ in terms of conditions in the outlet plane. From conservation of momentum in the tangential direction (fig. 6),

$$\int_{-Y}^{Y} \rho V_{z,x} V_{y,x} dy = 2Y\rho V_{z,\infty} V_{y,\infty} \tag{A3}$$

Using the relation $V_y = V_z \tan\beta$, equation (A3) becomes

$$\tan\beta_\infty = \frac{\tan\beta_x \int_{-Y}^{Y} V_{z,x}^2 dy}{2YV_{z,\infty}^2}$$

Therefore,

$$\cos \beta_\infty = \frac{2YV_{z,\infty}^2}{\sqrt{\left(2YV_{z,\infty}^2\right)^2 + \tan^2\beta_x\left(\int_{-Y}^{Y} V_{z,x}^2 dy\right)^2}} \tag{A4}$$

For the conservation of mass flow,

$$\int_{-Y}^{Y} \rho V_{z,x} dy = 2Y\ \rho V_{z,\infty}$$

or

$$V_{z,\infty} = \frac{V_{0,x}\cos\ \beta_x}{2Y} \int_{-Y}^{Y} \left(\frac{V_x}{V_{0,x}}\right) dy = \frac{V_{0,x}\cos\ \beta_x}{2Y} \left[2Y - \int_{-\delta_{l,y}}^{\delta_{u,y}} \left(1 - \frac{V_x}{V_{0,x}}\right) dy\right] \tag{A5}$$

Then, in terms of boundary-layer characteristics,

$$V_{z,\infty} = V_{0,x}\cos\ \beta_x \left(1 - \frac{\delta_y^*}{2Y}\right)_x \tag{A6}$$

Substitution of equations (A4) and (A6) into equation (A2) gives

$$(\Delta P)_\infty = \tfrac{1}{2}\ \rho V_{0,x}^2 + \tfrac{1}{2}\ \rho V_{0,x}^2 \left(1 - \frac{\delta_y^*}{2Y}\right)_x^2 \cos^2\beta_x \left\{1 - \frac{\tan^2\beta_x\left(\int_{-Y}^{Y} V_{z,x}^2 dy\right)^2}{\left[2YV_{0,x}^2\left(1 - \frac{\delta_y^*}{2Y}\right)_x^2 \cos^2\beta_x\right]^2}\right\} - \frac{1}{2Y}\int_{-Y}^{Y} \rho V_{z,x}^2 dy$$

or, factoring out $\frac{1}{2}\rho V_{0,x}^2$,

$$(\Delta P)_\infty = \frac{1}{2}\rho V_{0,x}^2 \left(1 + \left(1 - \frac{\delta_y^*}{2Y} \right)_x^2 \cos^2\beta_x \left\{ 1 - \frac{\tan^2\beta_x \left[\int_{-Y}^{Y} \left(\frac{V_{z,x}}{V_{0,x}} \right)^2 dy \right]^2}{(2Y)^2 \left(1 - \frac{\delta_y^*}{2Y} \right)_x^4 \cos^4\beta_x} \right\} - \frac{1}{Y} \int_{-Y}^{Y} \left(\frac{V_{z,x}}{V_{0,x}} \right)^2 dy \right) \tag{A7}$$

Now,

$$\int_{-Y}^{Y} \left(\frac{V_{z,x}}{V_{0,x}} \right)^2 dy = \int_{-\delta_{l,y}}^{\delta_{u,y}} \left(\frac{V_x}{V_{0,x}} \right)^2 \cos^2\beta_x dy$$

$$= \cos^2\beta_x \left\{ 2Y - \int_{-\delta_{l,y}}^{\delta_{u,y}} \left[1 - \left(\frac{V_x}{V_{0,x}} \right)^2 \right] dy \right\}$$

$$= \cos^2\beta_x \left[2Y - \int_{-\delta_{l,y}}^{\delta_{u,y}} \left(1 - \frac{V_x}{V_{0,x}} \right) \left(\frac{V_x}{V_{0,x}} \right) dy - \int_{-\delta_{l,y}}^{\delta_{u,y}} \left(1 - \frac{V_x}{V_{0,x}} \right) dy \right]$$

$$= 2Y \cos^2\beta_x \left(1 - \frac{\theta_y}{2Y} - \frac{\delta_y^*}{2Y} \right)_x \tag{A8}$$

The expression of $V_{0,x}$ in terms of V_1 from equation (10) and the substitution of equation (A8) into equation (A7) then yields, after reducing,

$$(\Delta\bar{P})_\infty = \frac{\frac{1}{2}\rho V_1^2\left(\frac{\cos\beta_1}{\cos\beta_x}\right)^2}{\left[1-\left(\frac{\delta_y^*}{2Y}\right)_x\right]^2}\left\{\cos^2\beta_x\left(\frac{\delta_y^*}{2Y}\right)_x^2 - \frac{\sin^2\beta_x\left(\frac{\theta_y}{2Y}\right)_x^2}{\left[1-\left(\frac{\delta_y^*}{2Y}\right)_x\right]^2} + \frac{2\sin^2\beta_x\left(\frac{\theta_y}{2Y}\right)_x}{1-\left(\frac{\delta_y^*}{2Y}\right)_x} + 2\cos^2\beta_x\left(\frac{\theta_y}{2Y}\right)_x\right\} \quad \text{(A9)}$$

With the use of equations (14) and the definitions of solidity, form factor H, and momentum-thickness parameter $\hat{\theta}$ (eq. (19)), equation (A9) can be expressed in terms of the loss coefficient $\bar{\omega}^*_{\infty,x}$, defined by equation (22), as

$$\bar{\omega}^*_{\infty,x} = \frac{2\hat{\theta}_x}{(1-\hat{\theta}_x H_x)^2}\left\{\cos^2\beta_x + \frac{\sin^2\beta_x}{(1-\hat{\theta}_x H_x)} + \frac{\hat{\theta}_x}{2}\left[H_x^2\cos^2\beta_x - \frac{\sin^2\beta_x}{(1-\hat{\theta}_x H_x)^2}\right]\right\} \quad \text{(A10)}$$

With the use of the identity $\cos^2\beta = 1 - \sin^2\beta$, equation (A10) becomes

$$\bar{\omega}^*_{\infty,x} = \frac{2\hat{\theta}_x}{(1-\hat{\theta}_x H_x)^2}\left[1 + \frac{\hat{\theta}_x H_x}{1-\hat{\theta}_x H_x}\sin^2\beta_x + \frac{\hat{\theta}_x H_x^2}{2} - \frac{\hat{\theta}_x H_x^2}{2}\sin^2\beta_x - \frac{\hat{\theta}_x\sin^2\beta_x}{2(1-\hat{\theta}_x H_x)^2}\right]$$

Factoring and reducing of terms then yields for the loss coefficient for complete mixing

$$\bar{\omega}^*_{\infty,x} = \frac{2\hat{\theta}_x}{(1-\hat{\theta}_x H_x)^2}\left\{1 + \frac{\hat{\theta}_x}{2}\left[H_x^2 - \sin^2\beta_x\left(H_x - \frac{1}{1-\hat{\theta}_x H_x}\right)^2\right]\right\} \quad (23)$$

REFERENCES

1. Thwaites, B.: Approximate Calculation of the Laminar Boundary Layer. Aero. Quart., vol. 1, Nov. 1949, pp. 245-280.

2. Maskell, E. C.: Approximate Calculation of the Turbulent Boundary Layer in Two-Dimensional Incompressible Flow. Rep. No. Aero. 2443, British R.A.E., Nov. 1951.

3559

3. Stewart, Warner L.: Analysis of Two-Dimensional Compressible-Flow Characteristics Downstream of Turbomachine Blade Rows in Terms of Basic Boundary-Layer Characteristics. NACA TN 3515, 1955.

4. Schlichting, H., and Scholz, N.: Über die theoretische Berechnung der Strömungsverluste eines ebenen Schaufelgitters Ing.-Archiv, Bd. XIX, Heft 1, 1951, pp. 42-65.

5. McGregor, Charles A.: Two-Dimensional Losses in Turbine Blades. Jour. Aero. Sci., vol. 19, no. 6, June 1952, pp. 404-408.

6. Schlichting, Herman: Problems and Results of Investigations on Cascade Flow. Jour. Aero. Sci., vol. 21, no. 3, Mar. 1954, pp. 163-178.

7. Thurston, Sidney, and Brunk, Ralph E.: Performance of a Cascade in an Annular Vortex-Generating Tunnel over Range of Reynolds Numbers. NACA RM E51F30, 1951.

8. Winter, K. G.: Comparative Tests of Thick and Thin Turning Vanes in the 4 ft. × 3 ft. Wind Tunnel. Rep. No. Aero. 2217, British R.A.E., Aug. 1947.

9. Briggs, William B.: Effect of Mach Number on the Flow and Application of Compressibility Corrections in a Two-Dimensional Subsonic-Transonic Compressor Cascade Having Varied Porous-Wall Suction at the Blade Tips. NACA TN 2649, 1952.

10. Bowen, J. T., Sabersky, R. H., and Rannie, W. D.: Investigations of Axial-Flow Compressors. A.S.M.E. Trans., vol. 73, no. 1, Jan. 1951, pp. 1-14.

11. Reeman, J., and Simonis, E. A.: The Effect of Trailing Edge Thickness on Blade Loss. Tech. Note No. 116, British R.A.E., Mar. 1943.

12. Preston, J. H., and Sweeting, N. E.: The Experimental Determination of the Boundary Layer and Wake Characteristics of a Simple Joukowski Aerofoil, with Particular Reference to the Trailing Edge Region. R. & M. No. 1998, British A.R.C., 1943.

13. Preston, J. H. Sweeting, N. E., and Cox, D. K.: The Experimental Determination of the Boundary Layer and Wake Characteristics of a Piercy 12/40 Aerofoil, with Particular Reference to the Trailing Edge Region. R. & M. No. 2013, British A.R.C., Feb. 26, 1945.

TABLE I. - EQUATIONS FOR V/V_0, K, AND θ FOR ANALYTICAL WAKE VELOCITY PROFILES OF FIGURE 3

Wake profile	Velocity ratio, V/V_0	Pseudoenergy factor, K	Momentum thickness, θ
(a) Power	$\left(\frac{2y}{\delta}\right)^n$	$\frac{H+1}{3H-1}$	$\frac{1}{H}\left(\frac{H-1}{H+1}\right)\delta$
(b) Linear	$\frac{V_{min}}{V_0} + \left(1 - \frac{V_{min}}{V_0}\right)\frac{2y}{\delta}$	$\frac{H^2 - 2H + 9}{8H}$	$\frac{3}{4}\left(\frac{H-1}{H^2}\right)\delta$
(c) Half-sine wave	$\frac{1}{2}\left[\left(1 + \frac{V_{min}}{V_0}\right) - \left(1 - \frac{V_{min}}{V_0}\right)\cos\left(\pi\frac{2y}{\delta}\right)\right]$	$\frac{H^2 - 2H + 10}{9H}$	$\frac{2}{3}\left(\frac{H-1}{H^2}\right)\delta$
(d) Quarter-sine wave	$\frac{V_{min}}{V_0} + \left(1 - \frac{V_{min}}{V_0}\right)\sin\left(\pi\frac{y}{\delta}\right)$	$\frac{1}{H}\left[(a-1)H^2 - 2(a-1)H + a\right]$ $a = \frac{2}{3}\frac{(15\pi - 44)(\pi - 2)}{(3\pi - 8)^2}$	$\frac{2}{\pi}\frac{(\pi-2)^2}{3\pi - 8}\left(\frac{H-1}{H^2}\right)\delta$
(e) Error curve	$1 - \left(1 - \frac{V_{min}}{V_0}\right)e^{-b\left(\frac{2y}{\delta}\right)^2}$ $b = \ln\left[100\left(1 - \frac{V_{min}}{V_0}\right)\right]$	$\frac{1}{H}\left[(a-1)H^2 - 2(a-1)H + a\right]$ $a = \frac{2}{\sqrt{3}}$	$\sqrt{\frac{\pi}{2b}}\left(\frac{H-1}{H^2}\right)\delta$ $b = \ln\left[100\sqrt{2}\left(\frac{H-1}{H}\right)\right]$

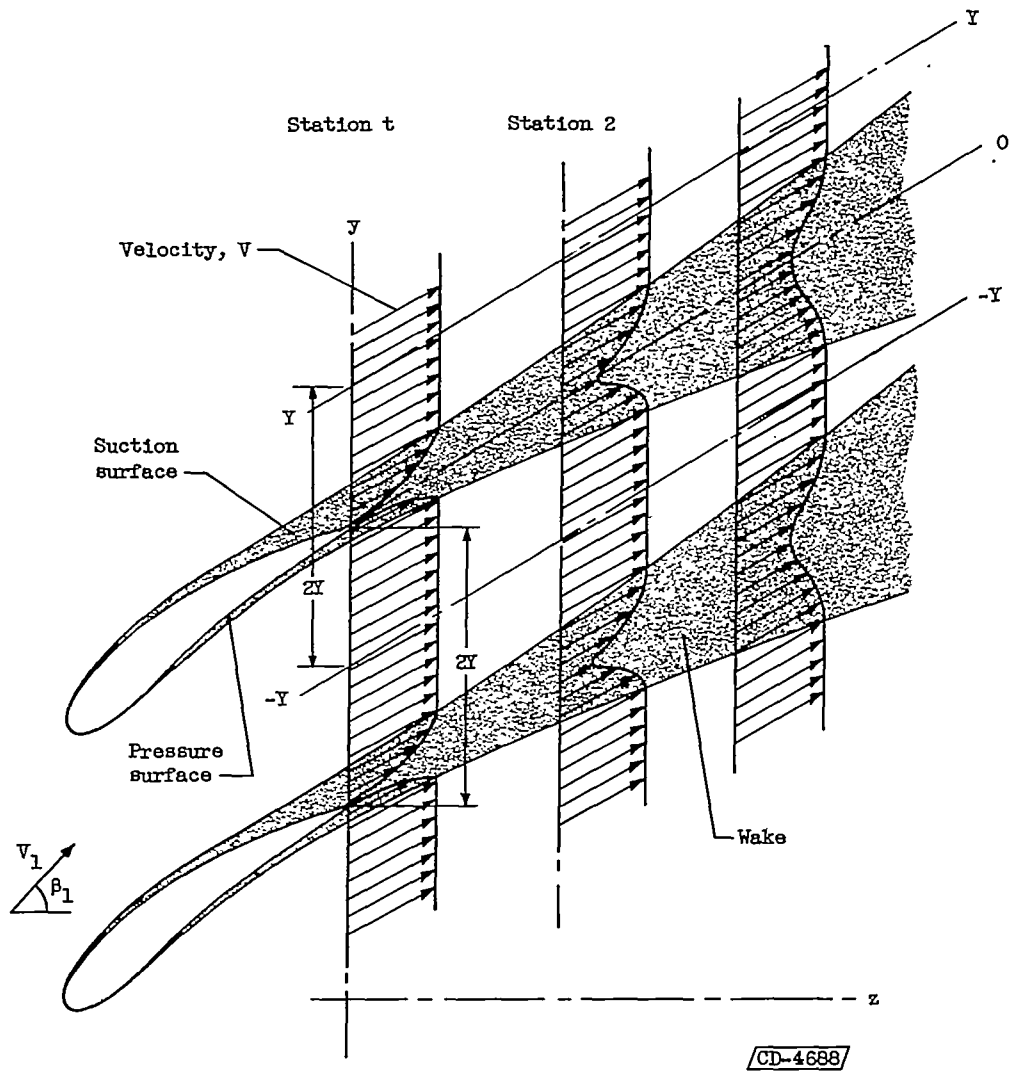

Figure 1. - Development of surface boundary layers and wake in flow about cascade blade sections as considered by loss analysis.

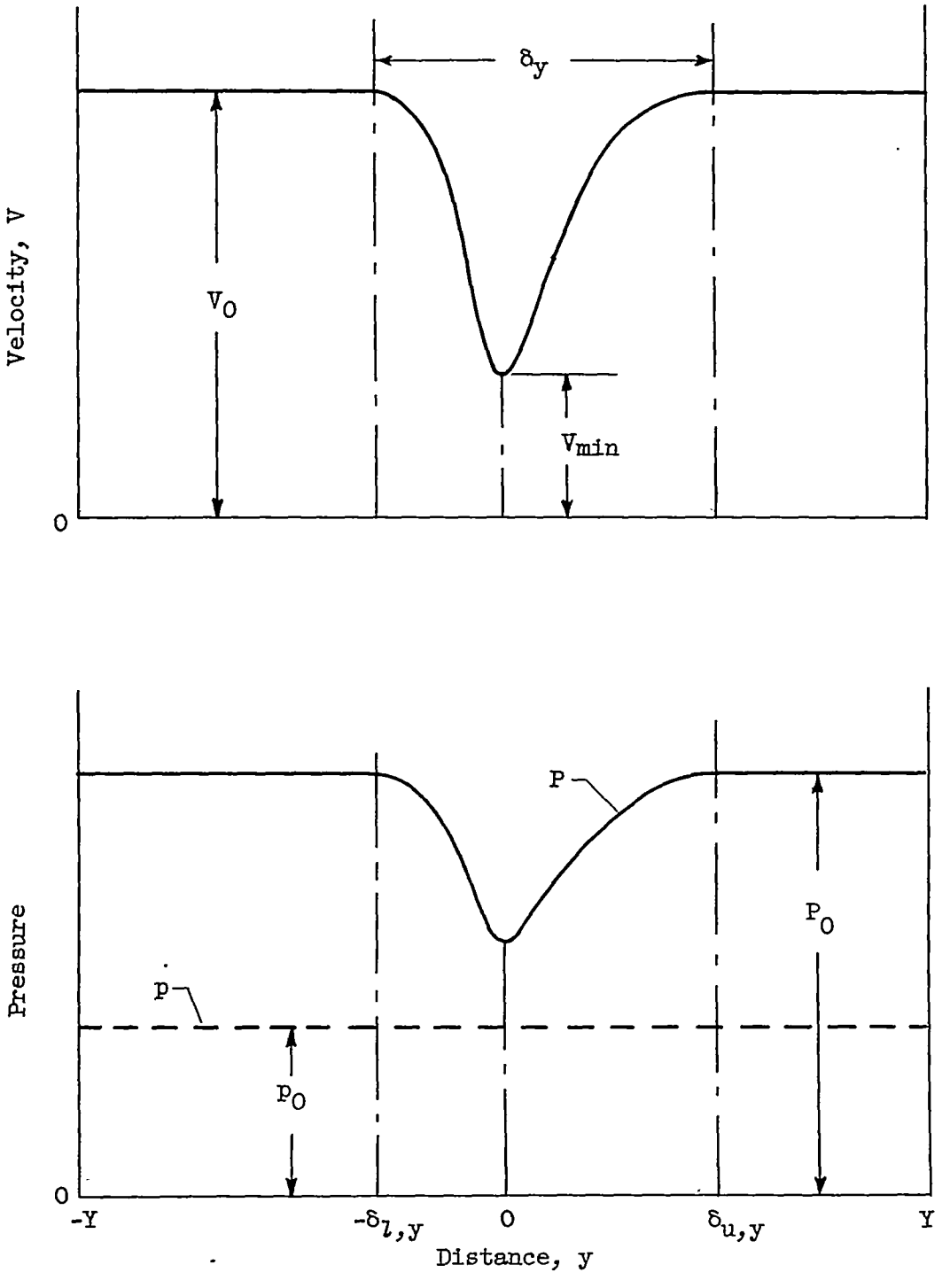

Figure 2. - Model variation of velocity and pressure in plane normal to axis at arbitrary station downstream of cascade as used in loss analysis.

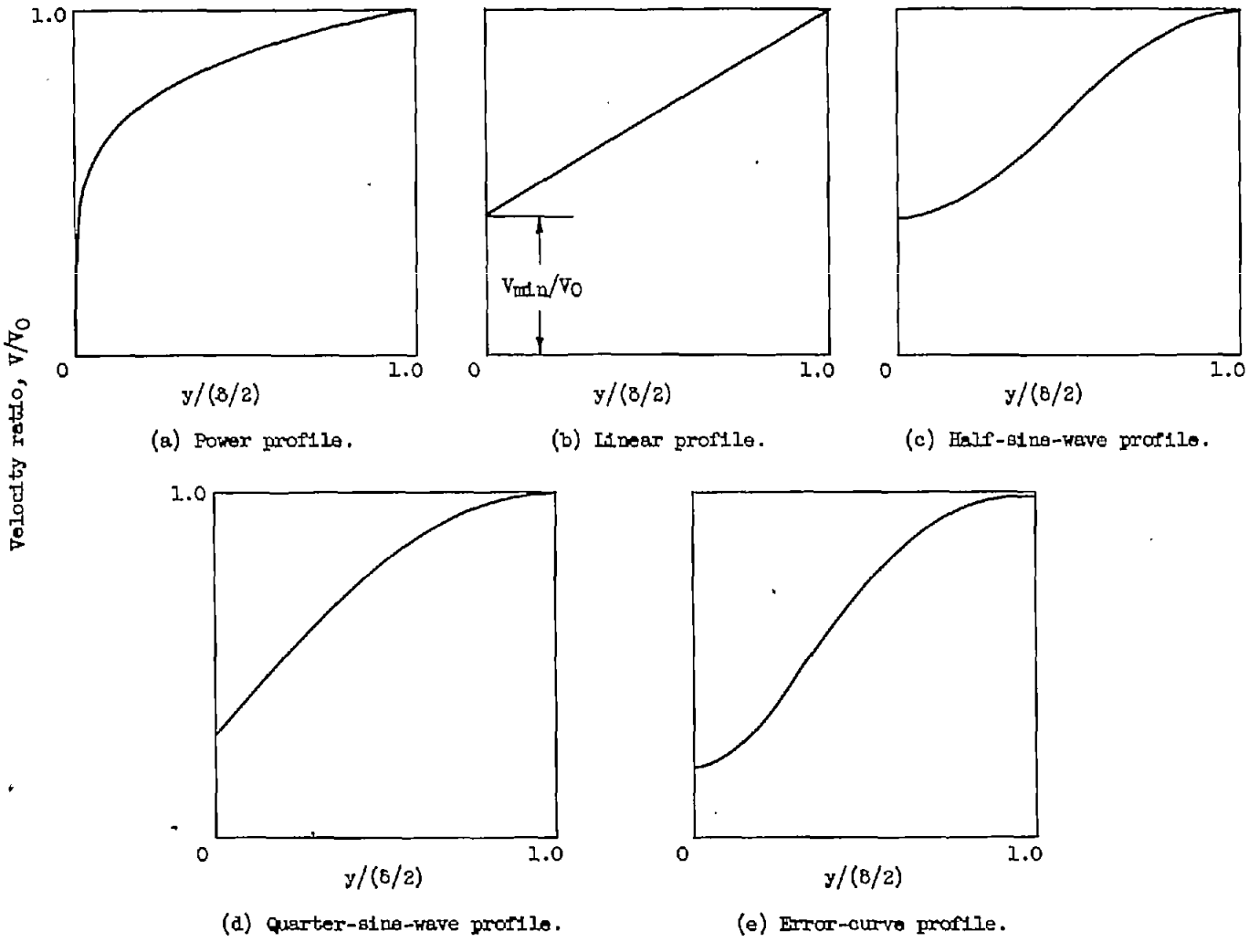

(a) Power profile. (b) Linear profile. (c) Half-sine-wave profile.

(d) Quarter-sine-wave profile. (e) Error-curve profile.

Figure 3. - Analytical velocity profiles in half wake used in analysis of wake properties.

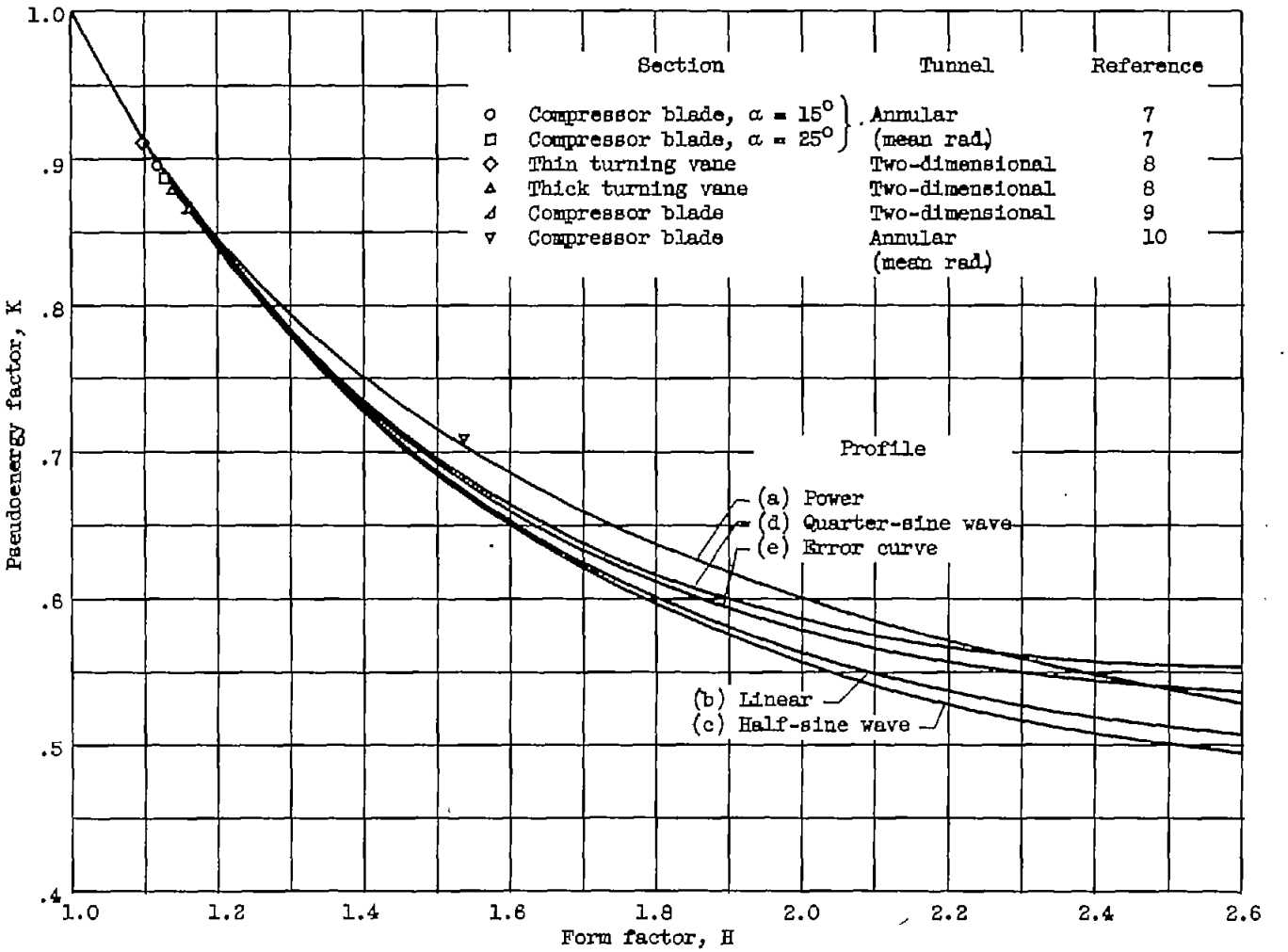

Figure 4. - Calculated variation of pseudoenergy factor with form factor for representative analytical wake velocity profiles of figure 3. Values computed from experimental wake data are also shown.

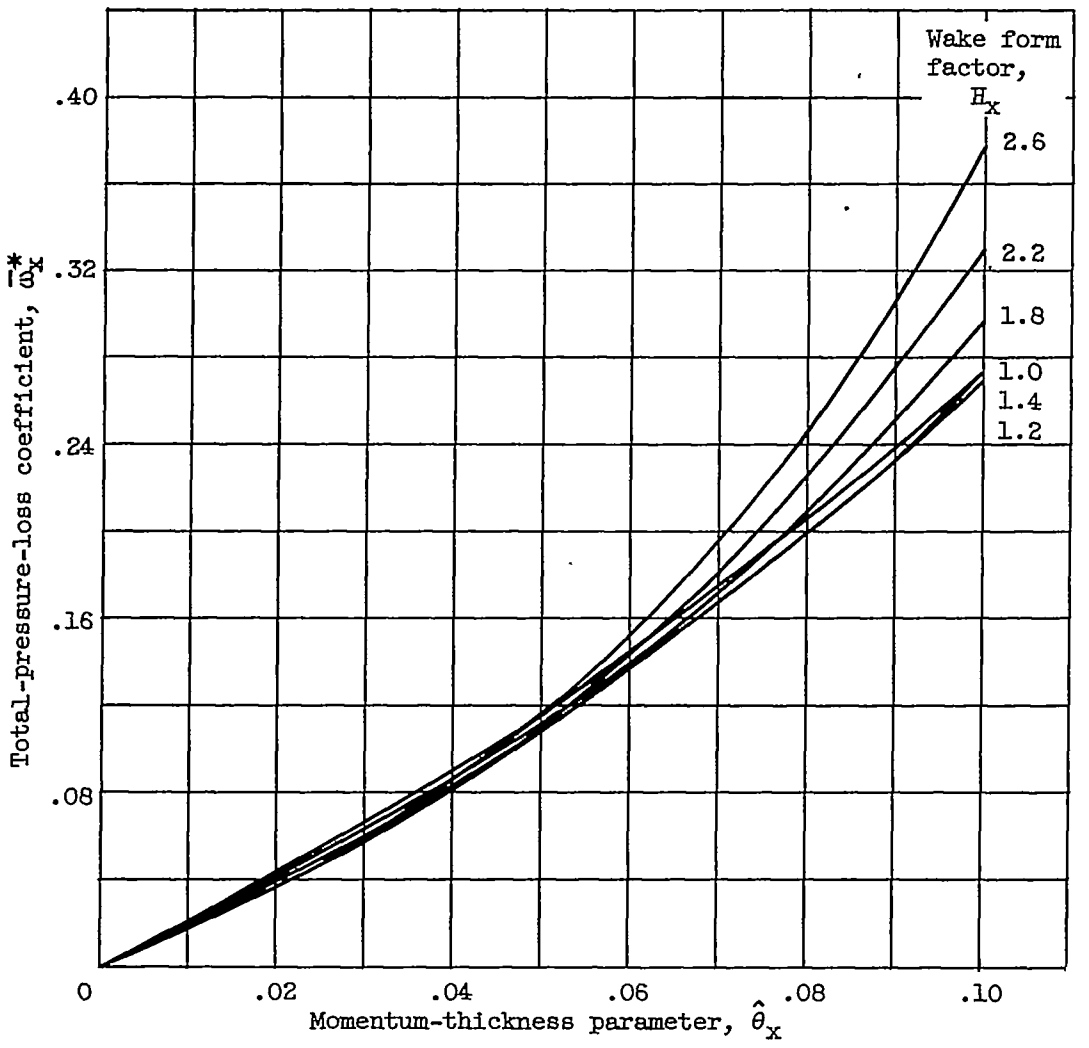

Figure 5. - Theoretical variation of total-pressure-loss coefficient in outlet plane with wake momentum-thickness parameter in outlet plane.

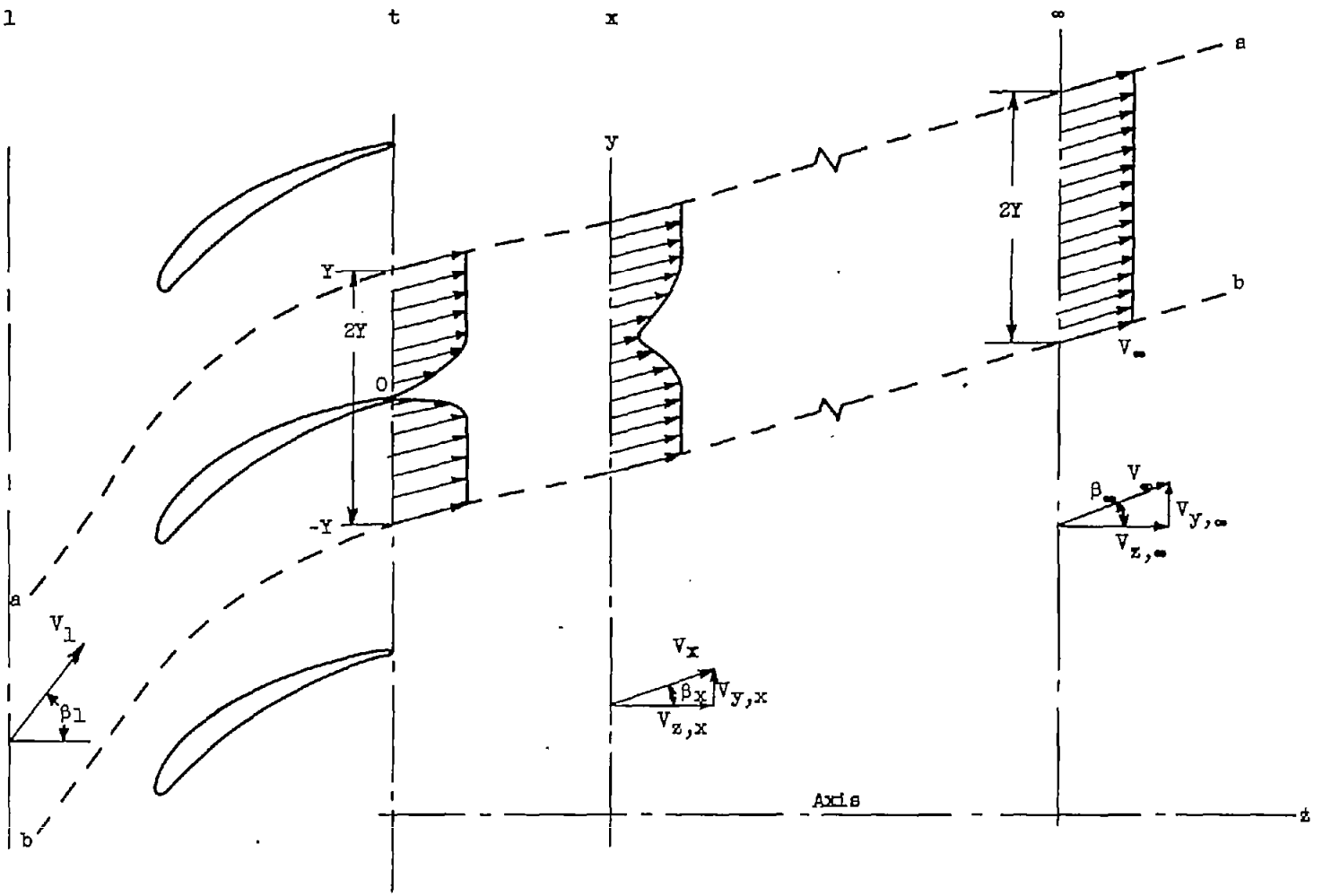

Figure 6. - Velocity variation close behind cascade and far downstream where complete mixing has taken place. a-a and b-b are streamlines for full blade spacing 2Y.

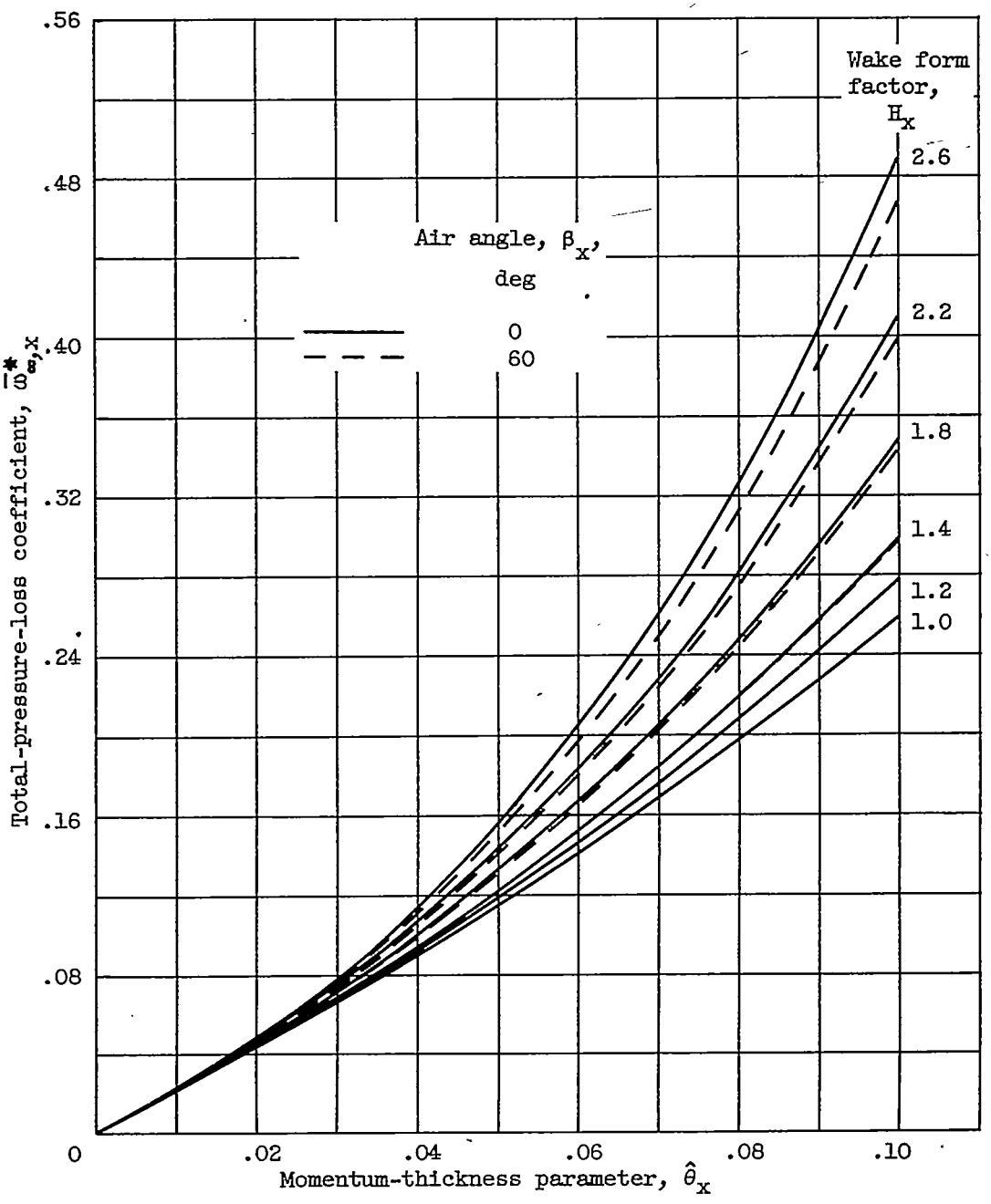

Figure 7. - Theoretical variation of total-pressure-loss coefficient for complete mixing with wake momentum-thickness parameter in outlet plane.

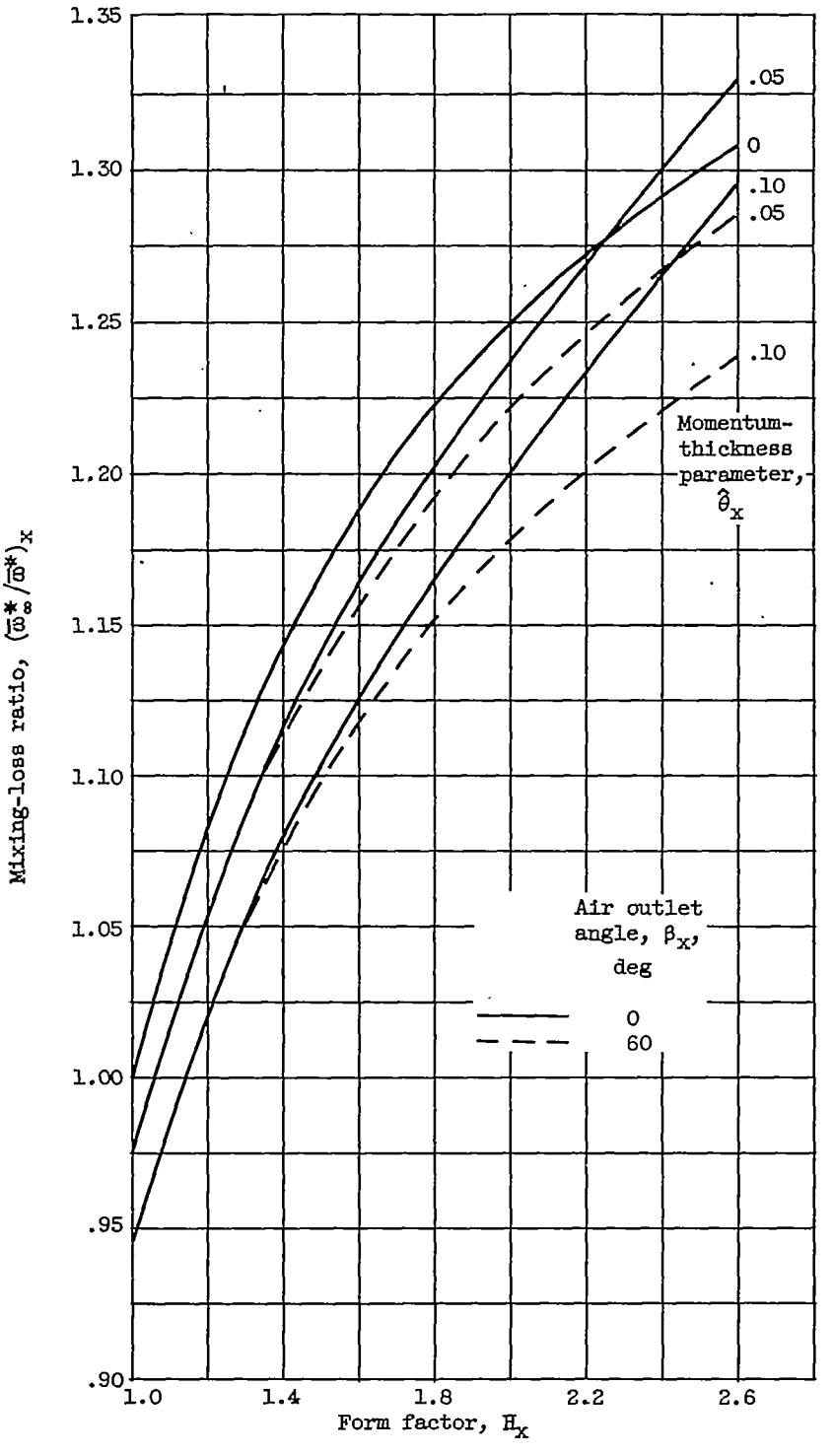

Figure 8. - Variation of theoretical mixing-loss ratio with wake form factor for various values of wake momentum-thickness parameter. (Values of mixing-loss ratio are the same for $\beta = 0^\circ$ and 60° at $\hat{\theta}_x = 0$.)

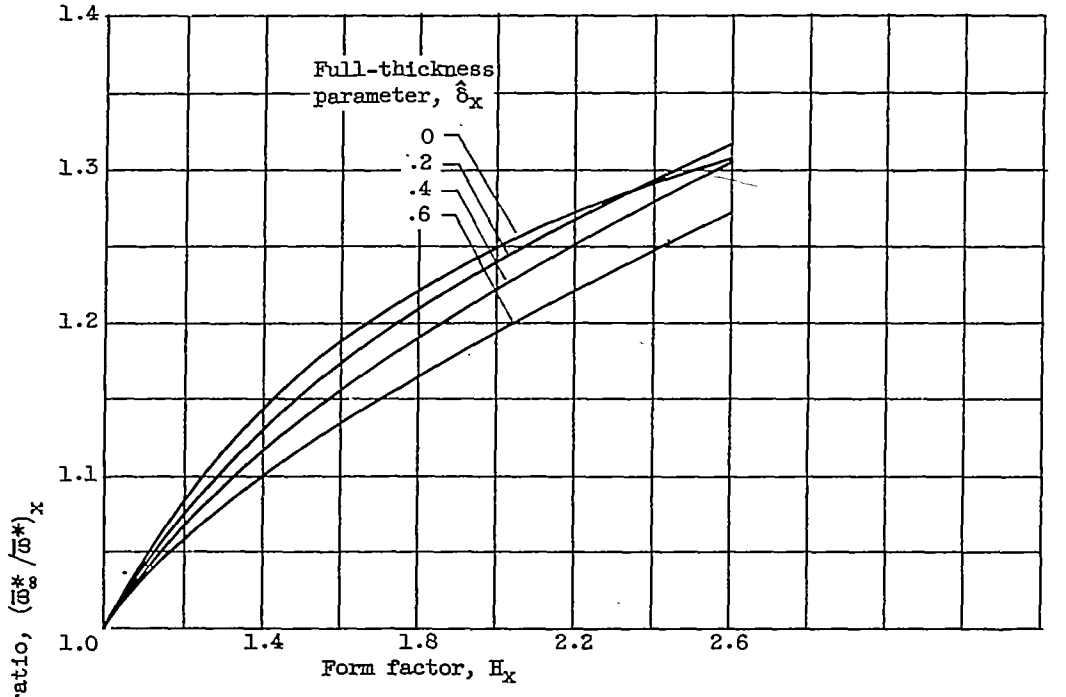

(a) Variation with form factor; $\beta_x = 30^\circ$.

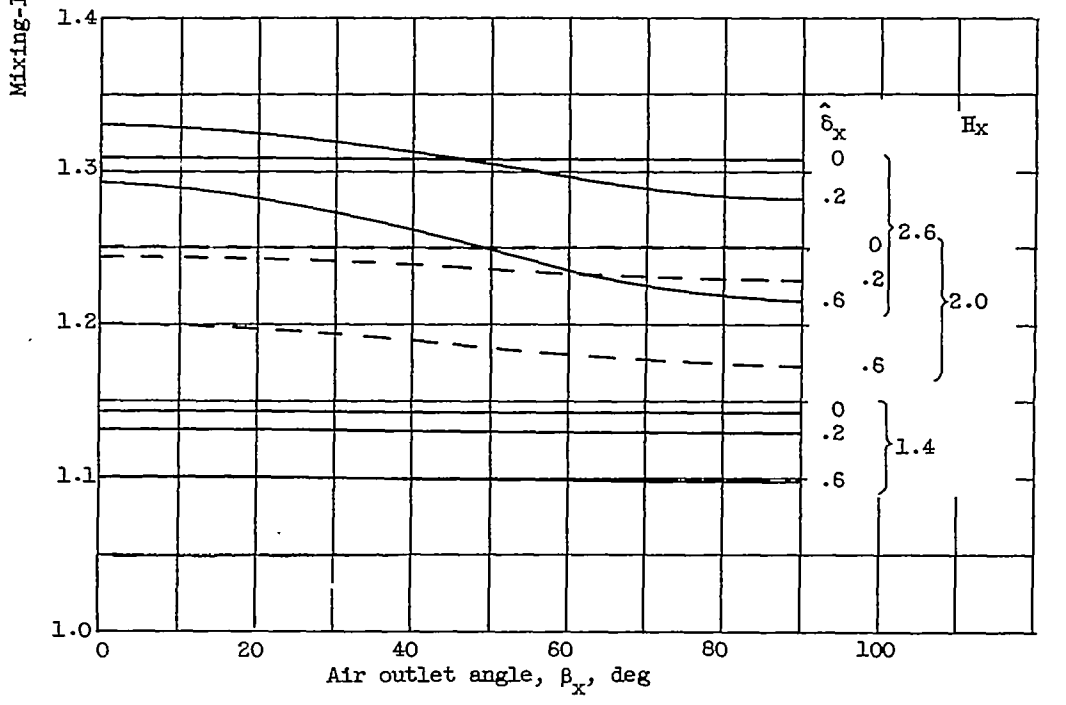

(b) Variation with air outlet angle.

Figure 9. - Theoretical mixing-loss ratio for power velocity profile in wake.

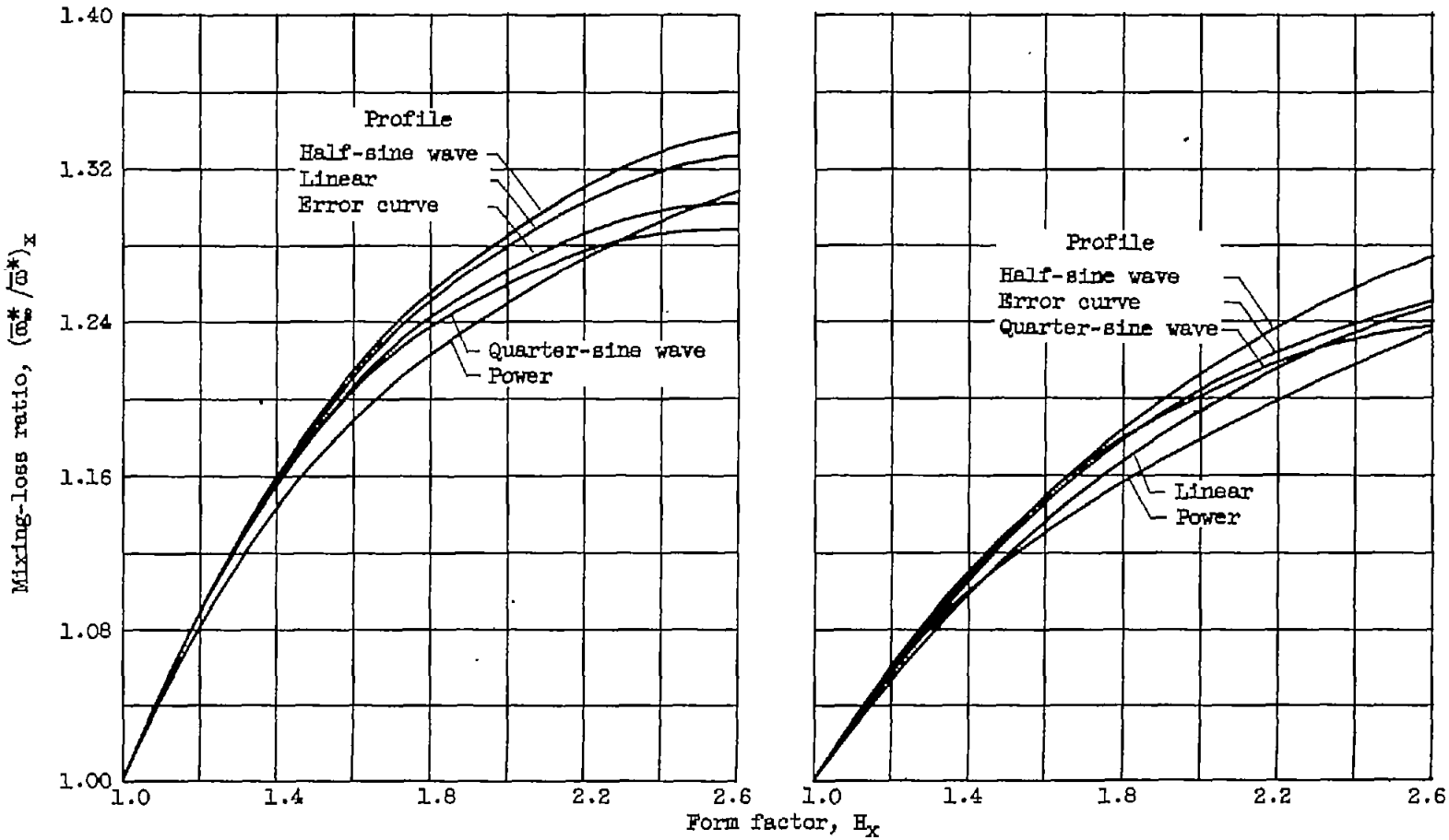

(a) Full-thickness parameter, $\hat{\delta}_x$, 0 (all values of β_x).

(b) Full-thickness parameter, $\hat{\delta}_x$, 0.6; β_x, 60°.

Figure 10. - Effect of wake velocity profile on theoretical mixing-loss ratio.

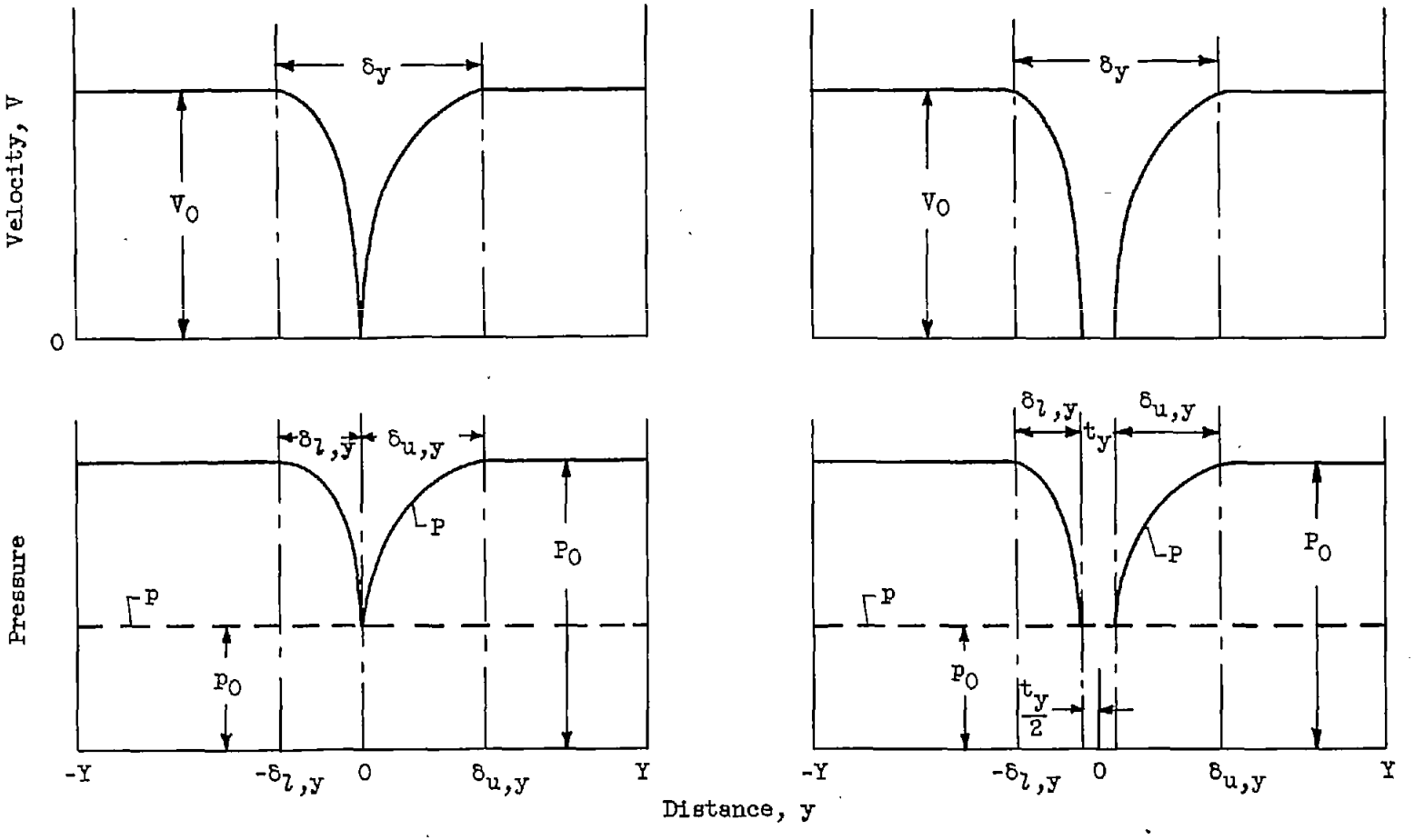

(a) Zero blade trailing-edge thickness.

(b) Nonzero blade trailing-edge thickness; $t_y = t/\cos \beta_t$.

Figure 11. - Model variations of velocity and pressure in plane of trailing edge.

3559

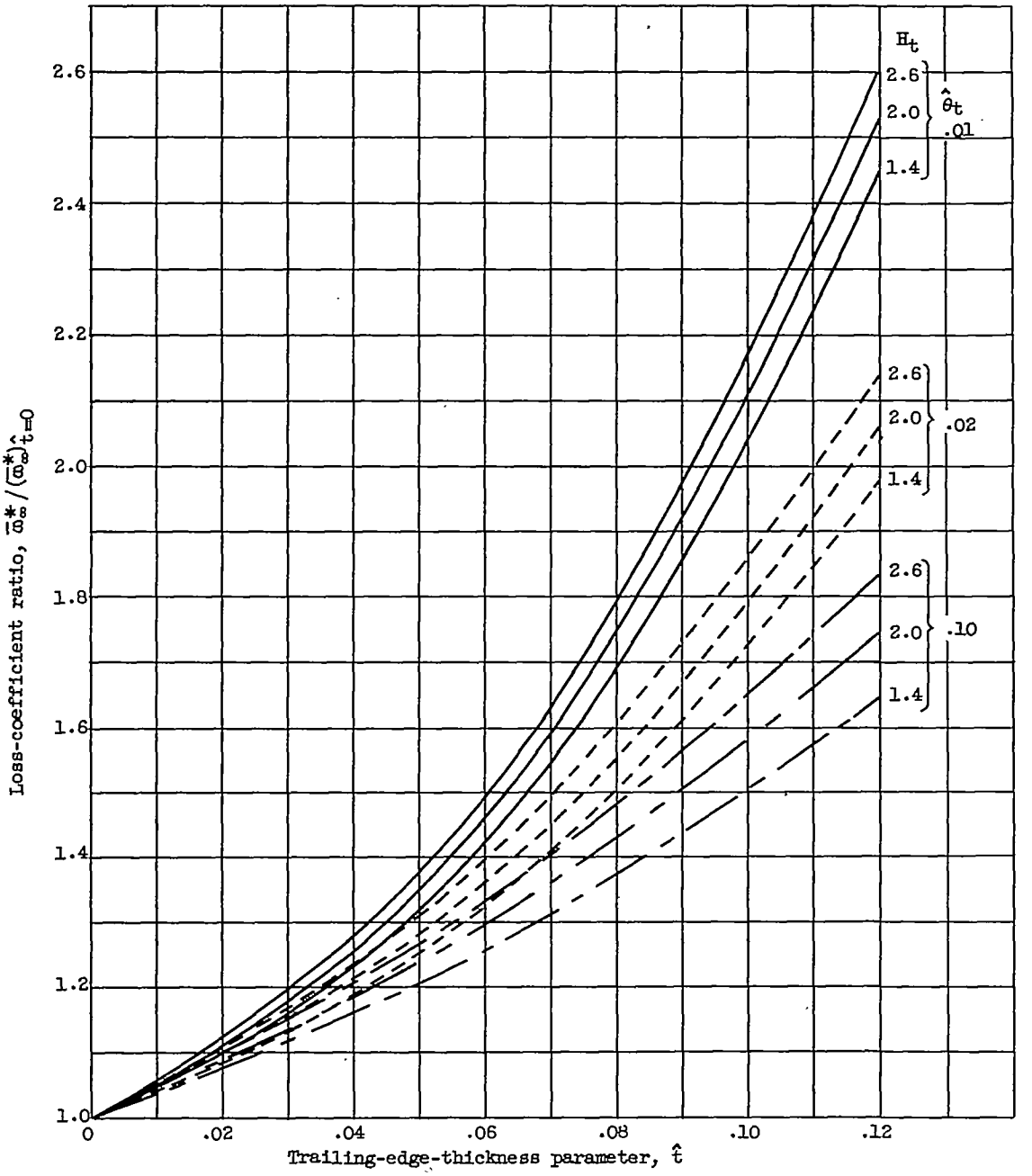

Figure 12. - Theoretical effect of blade trailing-edge thickness on total-pressure-loss coefficient for complete mixing.

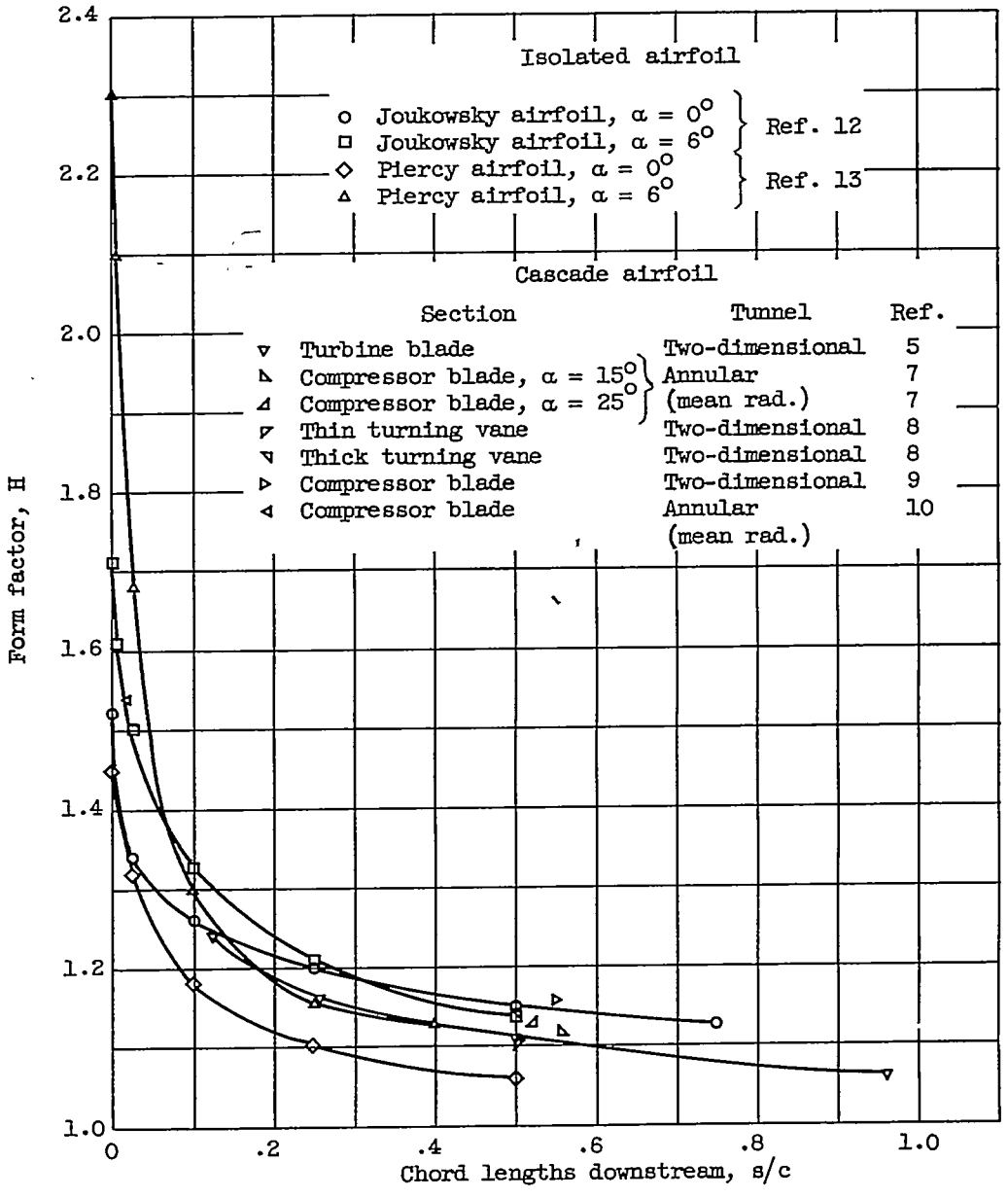

Figure 13. - Experimental variation of wake form factor with distance downstream of blade trailing edge.